



A fluorine scan of non-peptidic inhibitors of neprilysin: Fluorophobic and fluorophilic regions in an enzyme active site

Martin Morgenthaler^a, Johannes D. Aebi^b, Fiona Grüninger^b, Daniel Mona^b, Björn Wagner^b, Manfred Kansy^b, François Diederich^{a,*}

^a Laboratorium für Organische Chemie, ETH Zürich HCI, Hönggerberg, CH-8093 Zürich, Switzerland

^b Pharmaceuticals Division, Discovery Chemistry, F. Hoffmann-La Roche AG, CH-4070 Basel, Switzerland

ARTICLE INFO

Article history:

Received 26 January 2008

Received in revised form 19 February 2008

Accepted 19 February 2008

Available online 23 February 2008

Keywords:

Neprilysin

Fluorine interactions

Medicinal chemistry

pK_a value

Benzimidazole

ABSTRACT

This article describes the synthesis and *in vitro* biological affinities of (poly)fluorinated neprilysin inhibitors. Two series of inhibitors with F-substitution of the central benzimidazole platform of the ligands and the benzylic vector to fill the S1' pocket of NEP were investigated. The S1' pocket was found to be highly fluorophobic, and F-substitution led to significantly decreased binding affinities of inhibitors. This result is explained by electrostatically unfavorable close contacts of organic fluorine with the negatively polarized π -surfaces of surrounding aromatic amino acid side chains. In contrast, the protein environment around the benzimidazole platform, with three electropositive guanidinium side chains of Arg residues, was found to provide a fluorophilic environment. Overall, the data support that organic fluorine, with its high negative charge density prefers to orient into electropositive regions of receptor sites. pK_a measurements of fluorinated ligands provided several simple patterns for the prediction of pK_a values of benzimidazoles, important building blocks in medicinal chemistry.

© 2008 Elsevier B.V. All rights reserved.

1. Introduction

Neprilysin (NEP, EC 3.4.24.11) is a mammalian Zn^{II}-dependent, membrane-bound endopeptidase (type-II integral membrane protein), related to other mammalian metalloproteases such as the endothelin-converting enzymes (ECE-1 and ECE-2), KELL, and PEX [1,2]. It is involved in the metabolism of a number of regulatory peptides of the nervous, cardiovascular, inflammatory, and immune systems.

The enzyme was extracted for the first time in 1974 from rabbit kidney brush border [3]. It is found in various tissues, but most abundantly in the kidney [4]. Besides the wide distribution, it also has broad substrate specificity. The first substrates discovered were the pentapeptidic endorphins Leu- and Met-enkephalin and Substance P [5,6]. Among numerous other substrates [4,7], the cardiovascular peptide atrial natriuretic peptide (ANP) is the most familiar [8]. Furthermore, NEP plays an important role in various cancers. The downregulation of NEP in the lung by cigarette smoke may be casually related to the development of small-cell carcinomas [9,10]. Recently, it has been reported that NEP degrades both amyloid β -peptides 1–40 and 1–42, which play a pivotal role in Alzheimer's disease [11,12].

Since NEP cleaves ANP and enkephalins, it is a potential drug target. ANP reduces blood pressure by sodium excretion in the kidneys [8]. Selective NEP inhibitors are, therefore, possible anti-hypertensive agents, either alone or in combination with selective ACE (angiotensin-converting enzyme) inhibitors or as dual NEP/ACE inhibitors, so-called vaso-peptidase inhibitors [13–16]. Enkephalins act as endogenous painkillers in the central nervous system by binding to μ - and δ -opiate receptors [17]. Blocking NEP by a selective inhibitor leads to enhanced enkephalin concentrations *in vitro* and to antinociceptive activity in mice [18]. This suggests that selective inhibitors of NEP can act as new analgesic therapeutics [4].

After the structure of the extracellular domain (residues 52–749) of human NEP complexed with the metalloprotease inhibitor phosphoramidon was solved by X-ray crystallography at 2.1 Å resolution (PDB: 1DMT) [19], our group started the development of novel non-peptidic inhibitors of NEP by X-ray structure-based *de novo* design using the molecular modeling program MOLOC [20]. This strategy has been successfully pursued by us in a variety of medicinal chemistry projects [21–26]. These investigations [27–29] led to ligands featuring central benzimidazole- and imidazo[4,5-c]pyridine-type platforms, with inhibitory activities (IC₅₀ values; concentration at which 50% maximal initial velocity is observed) in the low nanomolar potency range. Here, we report on systematic introduction of fluorine into these classes of inhibitors with the aim to explore fluorine interactions at the active site of neprilysin [30]. A similar “fluorine scan” had previously been

* Corresponding author. Tel.: +41 44 632 2992; fax: +41 44 632 1109.

E-mail address: diederich@org.chem.ethz.ch (F. Diederich).

conducted for inhibitors of thrombin, a serine protease from the blood coagulation cascade [25,26,31,32]. The aims of such efforts are the identification of fluorophilic and fluorophobic regions in protein environments and the development of predictive skills for gaining binding potency and selectivity through selective introduction of organic fluorine into lead compounds [33–36].

2. Results and discussion

2.1. The active site of neprilysin complexed to a non-peptidic ligand

Compounds (+)-**1a**/(+)-**2a** with a central imidazo[4,5-c]pyridine platform and (+)-**1b**/(+)-**2b** with a benzimidazole scaffold were found to be potent inhibitors of NEP with IC₅₀ values in the nanomolar range (Table 1) [29]. In fact, their activities are actually higher than previously determined when optimized assay conditions, preventing oxidative thiol deterioration, are applied as in the present study (see below). Thus, ligand (+)-**1a** binds to NEP with an IC₅₀ value of 8 nM (Table 1). The predicted binding mode of (+)-**1a** was confirmed by X-ray crystallography (PDB code 1Y8J) and is shown in Fig. 1.

The thiolate residue of (+)-**1a** ligates to the Zn²⁺ ion, participating together with the side chains of Glu646, His587, and His583 in an ideal tetrahedral coordination pattern. The benzyl group fills the deep hydrophobic S1' pocket which is lined by Phe106, Ile558, Phe563, Met579, Val580, Val692, and Trp693. This pocket has been shown to accommodate large substituents, such as biphenyl residues [6,7,37,38]; however, changing phenyl (in (+)-

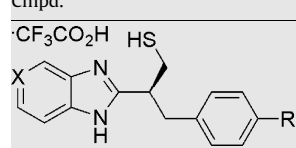
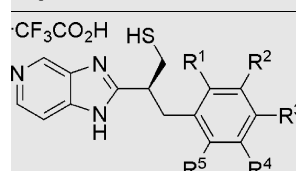
1a/(+)-**1b**) to biphenyl (in (+)-**2a**/(+)-**2b**) does not generate additional binding potency [29]. The imidazole ring of the central platform acts as peptide isoster [27] and forms H-bonds to the side chains of Arg717 and Asp542, while the annulated benzene/pyridine ring undergoes aromatic interactions with the side chains of His711 and Trp693. The crystal structure provides a good explanation for the measured enhanced binding affinity of the imidazo[4,5-c]pyridine-based ligands as compared to the benzimidazole derivatives (Table 1). In the complexes of (+)-**1b**/(+)-**2b**, two positively polarized H-atoms of the annulated benzene ring point to the positively charged side chain of Arg102, while in those of (+)-**1a**/(+)-**2a**, the N-atom of the annulated pyridine ring interacts with the guanidinium residue. However, at an N...N distance ≥3.7 Å, a possibly formed H-bond will only be very weak.

2.2. Exploring the S1' pocket: a distinct fluorophobic environment

Based on the finding that the S1' pocket of NEP accommodates a biphenyl substituent, as in (+)-**2a**/(+)-**2b**, albeit at no gain in binding potency [29], we wanted to further explore size and depth of this hydrophobic sub-site and in particular its affinity for organic fluorine. For this purpose, we prepared a series of enantiomerically pure inhibitors featuring alkyl and cycloalkyl ((+)-**4a–d**) besides trifluoromethyl ((+)-**3a**/(+)-**3b**) substituents in *para*-position of a benzyl ring to fill the pocket. Additionally, the benzylic ring was mono-, di-, and perfluorinated ((+)-**5a–j**).

The synthesis of all inhibitors followed the same route and is, with minor improvements, largely based on previously reported

Table 1
Biological activities of NEP inhibitors

Cmpd.	X	R	IC ₅₀ (nM)			
						
(+)- 1a	N	H	40 ^a /8			
(+)- 1b	CH	H	280 ^a /28			
(+)- 2a	N	Ph	34 ^a			
(+)- 2b	CH	Ph	300 ^a			
(+)- 3a	N	CF ₃	175			
(+)- 3b	CH	CF ₃	520			
(+)- 4a	N	CH ₃	90			
(+)- 4b	N	Cyclobutyl	120			
(+)- 4c	N	Cyclobutyl	320			
(+)- 4d	N	Cyclobutyl	170			
Cmpd.	R ¹	R ²	R ³	R ⁴	R ⁵	IC ₅₀ (nM)
						
(+)- 5a	H	H	F	H	H	160
(+)- 5b	H	F	H	H	H	170
(+)- 5c	F	H	H	H	H	180
(+)- 5d	H	F	F	H	H	340
(+)- 5e	F	H	F	H	H	220
(+)- 5f	F	F	H	H	H	210
(+)- 5g	F	H	H	F	H	220
(+)- 5h	F	H	H	H	F	260
(+)- 5i	H	F	H	F	H	170
(+)- 5j	F	F	F	F	F	430

IC₅₀ values (uncertainties ±10%) measured under optimized assay conditions are given in nM.

^a IC₅₀ values previously obtained using non-optimized assay conditions (see [29]).

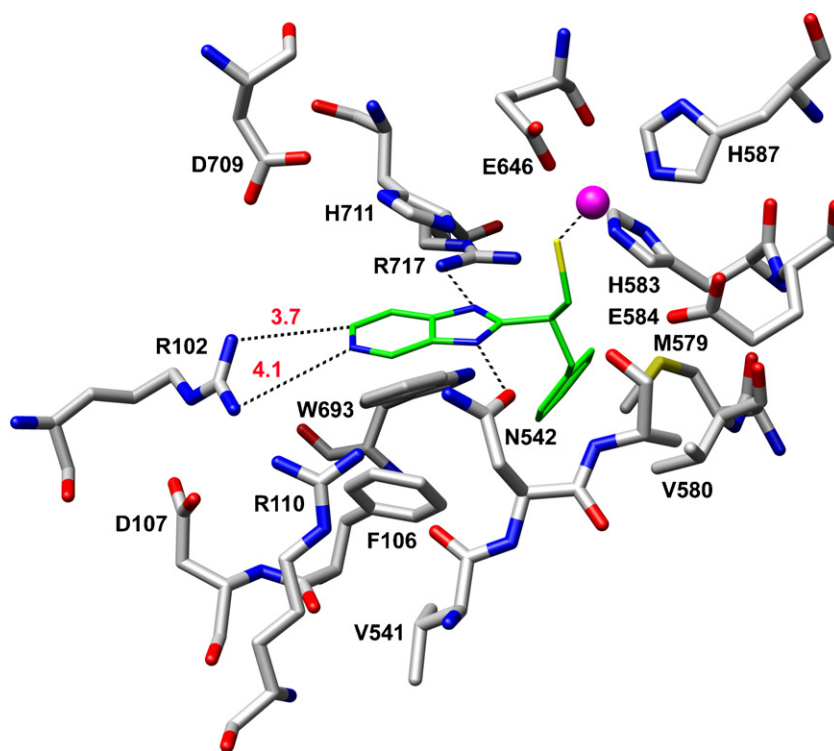
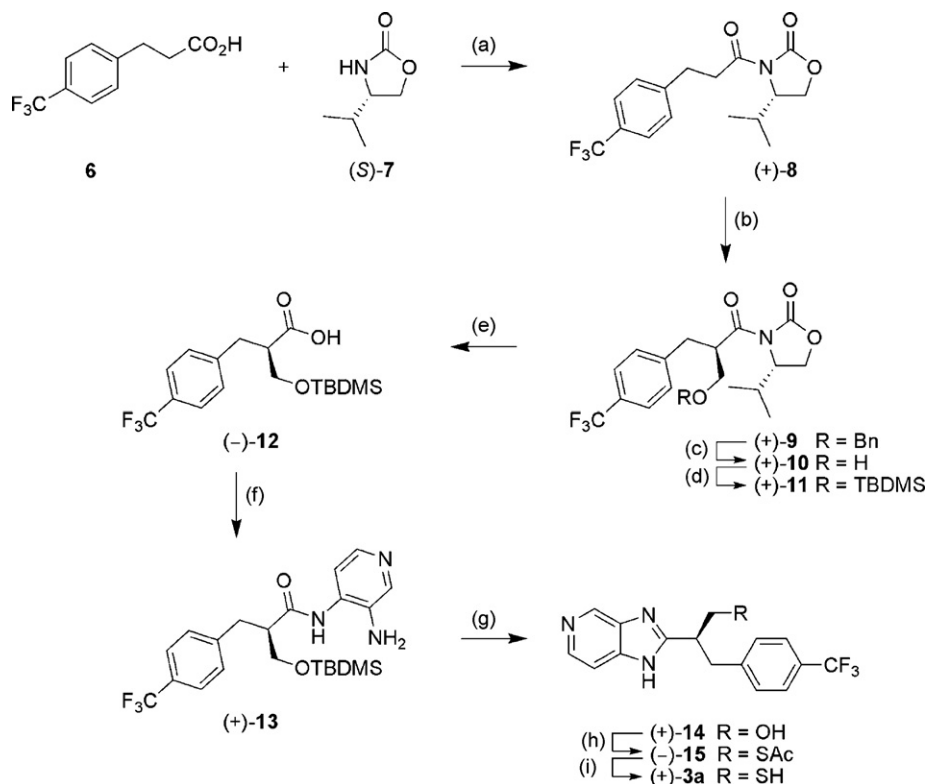


Fig. 1. Crystal structure of ligand (+)-**1a** complexed to NEP at a resolution of 2.25 Å [50]. PDB code 1Y8J [29]. Distances between N(5) and C(6) of the imidazo[4,5-c]pyridine platform to the N-atoms of the side chain of Arg102 are shown in Å. The bound ligand is shown as 3H-imidazo[4,5-c]pyridine tautomer; the other 1H-tautomer or a mixture of both could also be present. Color code—protein C-skeleton: grey; ligand C-skeleton: green; N-atoms: blue; O-atoms: red; S-atom: yellow; Zn²⁺ ion: pink ball. This color code also applies to the other figures where F-atoms are shown in pink.



Scheme 1. General synthesis sequence for fluorinated NEP inhibitors exemplified for (+)-**3a**. All other inhibitors were synthesized in an identical way. (a) (1) PivCl, Et₃N, THF, -30 °C, 90 min; (2) LiCl, (S)-**7**, r.t., 18 h, 68%. (b) (1) TiCl₄, (iPr)₂EtN, CH₂Cl₂, 0 °C, 1 h; (2) BOMCl, 0 °C, 3 h, 55%. (c) H₂, Pd/C, EtOAc, r.t., 24 h, 91%. (d) TBDMSCl, DMAP, CH₂Cl₂, r.t., 18 h, 99%. (e) H₂O₂, LiCl·H₂O, THF, H₂O, 0 °C, 3 h, r.t., 16 h, 90%. (f) (1) (COCl)₂, CH₂Cl₂, r.t., 12 h; (2) 3,4-diaminopyridine, Et₃N, THF, r.t., 12 h, 95%. (g) (1) AcOH, 65 °C, 24 h; (2) *n*Bu₄NF, THF, r.t., 2 h, 61%. (h) (1) PPh₃, DIAD, THF, 0 °C, 30 min; (2) AcSH, 0 °C, 1 h, r.t., 2 h, 75%. (i) NaOMe, H₂, MeOH, r.t., 2 h, 49%. Piv: pivaloyl; BOM: benzyloxymethyl; TBDMS: *t*-butyldimethylsilyl; DMAP: 4-(*N,N*-dimethylamino)pyridine; THF: tetrahydrofuran; Ac: acetyl; DIAD: diisopropylazodicarboxylate; r.t.: room temperature.

protocols [29]. The preparation of (+)-**3a** is exemplarily shown in Scheme 1. Hydrocinnamic acid derivative **6** was converted to a mixed anhydride with pivaloyl chloride and coupled *in situ* with the chiral *Evans* auxiliary (*S*)-**7** [39] to the acylated species (+)-**8**. Transformation into the corresponding Ti-enolate and diastereoselective alkylation with BOMCl gave (+)-**9** (for abbreviations, see scheme caption). Debenzylation to (+)-**10** and subsequent protection of the primary alcohol gave (+)-**11**. The chiral auxiliary was then removed by LiOOH to give carboxylic acid (–)-**12**, which was converted into the corresponding acid chloride and reacted *in situ* with 3,4-diaminopyridine to give (+)-**13**. Cyclocondensation in warm AcOH and deprotection with *n*Bu₄NF yielded primary alcohol (+)-**14**, which was then converted to (–)-**15** using *Mitsunobu* conditions with AcSH as nucleophile. Methanolysis of the thioacetate gave the free thiol (+)-**3a**, which was prone to oxidation to the corresponding disulfide. To prevent the formation of the disulfide, the reaction was carried out under an atmosphere of H₂. After workup, the crude thiol was immediately purified by reverse-phase (RP)-HPLC and isolated

as its trifluoroacetate salt, which did not oxidize even after several weeks being exposed to air.

The *in vitro* activity of this series of inhibitors towards NEP was determined in a fluorimetric assay (Table 1, for details see [27,40]). In addition, the previously reported inhibitors (+)-**1a** and (+)-**1b** (R = H) were retested [29]. The assay conditions were optimized by eliminating the previously used preincubation (1 h at 37 °C) of the prepared mixtures of inhibitor and NEP, before the substrate was added. It was reasoned that preincubation in neutral buffer solution facilitates the oxidation of the inhibitors to the corresponding disulfides. Using these optimized conditions, the IC₅₀ values of (+)-**1a** and (+)-**1b** were found to be significantly lower than previously reported (9 nM vs. 40 nM for (+)-**1a**, and 28 nM vs. 280 nM for (+)-**1b**) [29]. These findings demonstrate the ease with which our class of inhibitors is oxidized, and a rapid handling of them in neutral solution is highly beneficial.

The IC₅₀ values of inhibitors (+)-**4a–d** (90–320 nM), with 4-alkylbenzyl vectors to fill the S1' pocket, are all higher than expected, especially when compared to the previously published

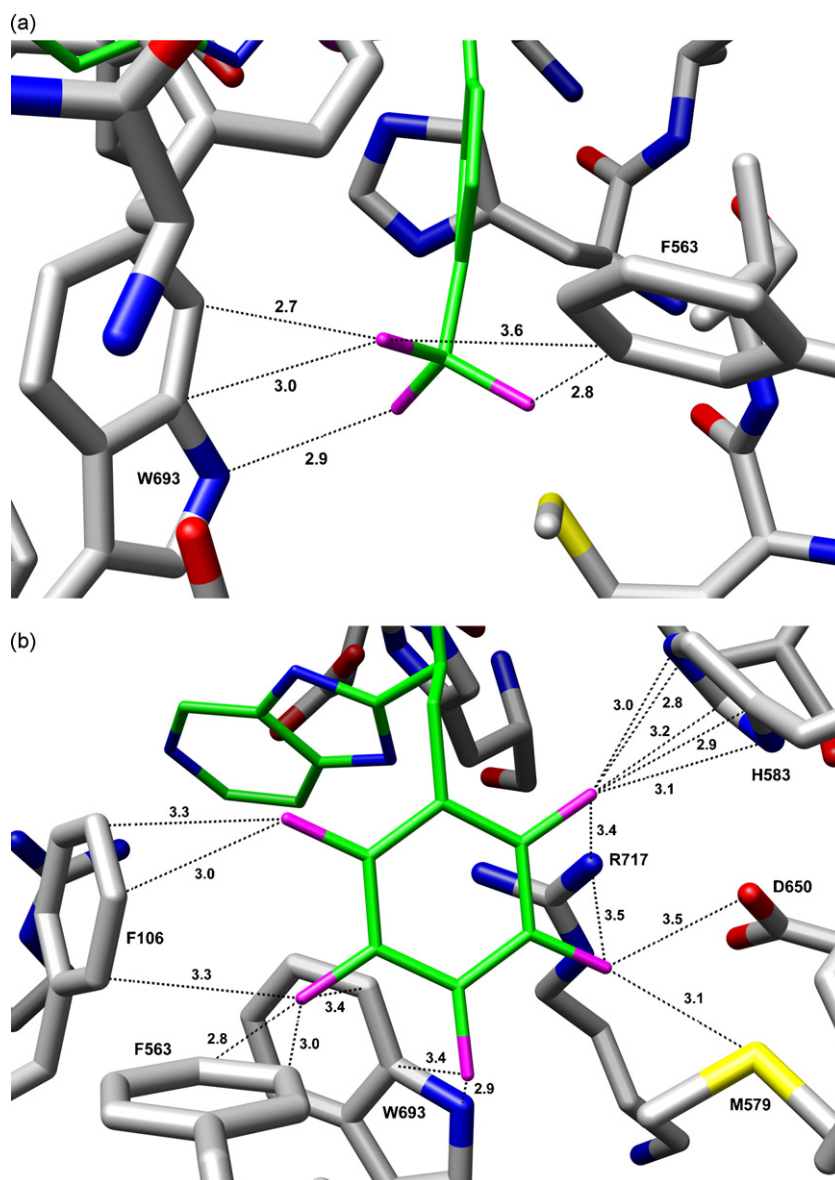


Fig. 2. Energy-minimized structures of (+)-**3a** (a) and (+)-**5j** (b) modeled in the active site of NEP. Short contacts between F atoms and side chains are indicated with dotted lines, the distances are given in Å. For the color code, see caption to Fig. 1.

values for the corresponding biphenyl substituted inhibitor (+)-**2a** (34 nM). The results suggest that the lower part of the S1' pocket is only filled without overall energetic losses by an aromatic substituent such as in biphenyl derivative (+)-**2a**. Molecular modeling indicates that the bottom of the S1' pocket actually is not that wide. Thus, the additional phenyl ring in the biphenyl derivatives (+)-**2a/b** undergoes repulsive contacts (as indicated by the program MOLOC) with the aromatic ring of Phe563 and the methyl group of the side chain of Met579. Additionally, a bound water molecule seen at the bottom of the pocket in the crystal structure of (+)-**1a** is displaced which could be energetically unfavorable. This water molecule is engaged in three hydrogen-bonding interactions with the indole nitrogen of Trp693 ($d(\text{N}\cdots\text{O}) = 2.9 \text{ \AA}$), with the backbone $\text{C}=\text{O}$ of Phe689 ($d(\text{O}\cdots\text{O}) = 3.0 \text{ \AA}$) and a second water molecule ($d(\text{O}\cdots\text{O}) = 2.7 \text{ \AA}$). This water molecule however does not seem to be conserved, as it is absent in other crystal structures (PDB codes 1R1I, 1R1J, 1DMT), and the energetics of its displacement are difficult to be estimated. On the other hand, the terminal phenyl ring in (+)-**2a/b** benefits from $S_{\text{Met579}}\cdots\pi$ interactions [41] and in particular from a favorable $\text{N}-\text{H}\cdots\pi$ interaction with the NH residue of the indole ring of Trp693 [42]. Overall, energetic gains and losses seem to balance out since the biphenyl derivatives (+)-**2a/b** are not more active than the benzyl derivatives (+)-**1a/b** (Table 1). In contrast, the alkylated derivatives (+)-**4a-d** do not benefit from specific aromatic interactions such as the NH/π interactions, but rather undergo several repulsive contacts only, which destabilize their complexes.

A remarkable destabilization of the complexes was also observed when organic fluorine was introduced into (+)-**1a/b**. Both the introduction of a CF_3 group into the *para*-position of the benzyl ring (in (+)-**3a/b**) as well as exchanging the hydrogen substituents of this ring by fluorine (in (+)-**5a-j**) led to substantially weaker binding, with IC_{50} values between 160 and 520 nM (as compared to 9 and 28 nM for (+)-**1a** and (+)-**1b**, respectively). Clearly, the S1' pocket of NEP constitutes a pronounced fluorophobic environment. The origin of the incompatibility for fluorine was further investigated by molecular modeling (Fig. 2).

This analysis suggests that the loss in binding potency originates from a too close proximity between the strongly negatively polarized F-atoms and electron-rich aromatic π -surfaces [43]. Thus, the CF_3 group in (+)-**3a** is surrounded by the aromatic side chains of Trp693 and Phe563 and the F-atoms point into the π -surfaces of the rings (Fig. 2a). The shortest distances

between F- and aromatic C-atoms are 2.7 and 3.0 Å (with Trp693), and 2.8 and 3.6 Å (Phe563), respectively. The only attractive interaction could be a weak, H-bond-type contact [30] between a fluorine of the ligand and NH of Trp693 (distance $\text{F}\cdots\text{N}$ of 2.9 Å). However, this interaction may not be very strong since the orientation of the N–H bond towards the F atom is not optimal. The IC_{50} value of the CF_3 derivative (+)-**3a** (175 nM) is by a factor of 2 higher than that of CH_3 -substituted (+)-**4a**. The actual loss in receptor–ligand binding affinity however is actually substantial, given the fact that introduction of the CF_3 moiety strongly enhances the lipophilicity (as expressed by the logarithmic coefficient $\log D$ for distribution (D) of a compound between octanol and water at pH 7.4) and thus promotes the transfer of the ligand from the aqueous solution into the protein, resulting in lower IC_{50} values [30,36,44]. A single H/F exchange usually renders $\log D$ more positive by 0.25 units.

Similarly, the F-atoms of (+)-**5a-j** undergo electrostatically unfavorable contacts with the surrounding electron-rich protein environment, as illustrated by the modeling shown in Fig. 2b. Thus, the fluorine substituents in pentafluorinated (+)-**5j** are in close contact with the π -electron surfaces of Phe106, Phe563, and His583 as well as with the electron-rich heteroatoms of the side chains of Asp650 and Met579.

It should be noted that the models shown in Fig. 2 are readily and reproducibly obtained by starting from the crystal structure of benzyl derivative (+)-**1a** (PDB code 1Y8J), adding the fluorine substituents to the NEP-bound ligand, and performing an energy minimization of the ligand while keeping the geometry of the protein fixed.

2.3. Exploring the surrounding of the benzimidazole platform: Arg residues provide a fluorophilic environment

The X-ray crystal structure of (+)-**1a** bound to NEP (Fig. 1) had suggested that the advantage of the imidazo[4,5-*c*]pyridine over the benzimidazole platform (e.g. (+)-**1a** vs. (+)-**2a**) resulted from favorable interactions of the N-lone pair of the annellated pyridine with the flexible side chain of Arg102. $\text{C}^{\delta+}-\text{F}^{\delta-}$ bonds can be viewed as bioisosteric replacements for heteroaromatic N-atoms with lone pairs [45]. Therefore, we explored whether F-substitution of the benzimidazole platform would enhance ligand affinity to NEP, since we expected the resulting C–F bonds to undergo favorable polar interactions with the electropositive guanidinium side

Table 2
Inhibitors of NEP with a fluorinated benzimidazole platform

Cmpd.	R ¹	R ²	R ³	R ⁴	IC ₅₀ (nM)	pK _{a1} ^a	pK _{a2} ^a
(+)- 16a	F	H	H	H	550	4.2	10.9
(+)- 16b	H	F	H	H	310	4.8	11.0
(+)- 16c	F	F	H	H	320	3.8	10.8
(+)- 16d	F	H	F	H	360	3.8	10.8
(+)- 16e	F	H	H	F	950	3.3	10.4
(+)- 16f	H	F	F	H	170	4.4	10.9
(+)- 16g	F	F	F	H	380	3.4	10.6
(+)- 16h	F	H	F	F	910	2.9	10.0
(+)- 16i	F	F	F	F	640	3.0	9.6
(+)- 3b	H	H	H	H	520	5.4	>12.0

IC₅₀ values (uncertainties ±10%) obtained under optimized assay conditions are given in nM.

^a The pK_a values were measured for precursor compounds with a CH_2OH instead of a CH_2SH group, in order to prevent interference of a third ionization step, involving thiol deprotonation. They are referred to in the text as (+)-**18** and (+)-**17a-i**.

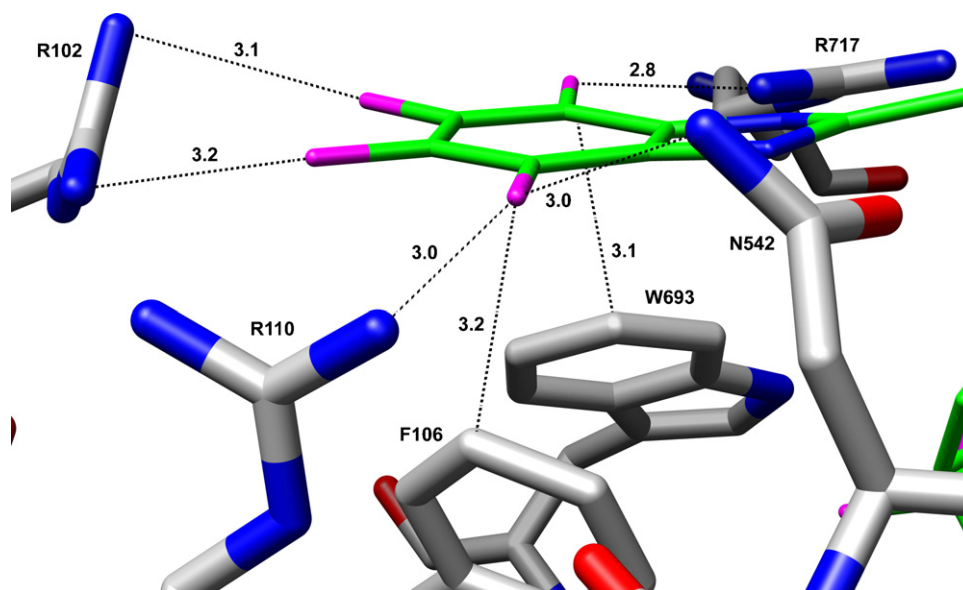


Fig. 3. Energy-minimized structure of (+)-**16i** modeled in the active site of NEP. Short contacts between F atoms and amino acid side chains are indicated with dotted lines, the distances are given in Å. For the color code, see caption to Fig. 1.

chains of Arg102, Arg110, and Arg717. While the position of Arg717 is highly conserved in the various X-ray crystal structures, the side chains of Arg102 and Arg110 are highly flexible and adopt various geometries in the presence of different classes of bound ligands [19,29,46]. For this purpose, we prepared inhibitors (+)-**16a–i** (Table 2), following the protocol shown in Scheme 1, which

all showed IC_{50} values in the upper nanomolar range for binding to NEP. It should be noted that this study and the earlier reported exploration of the S1' pocket were conducted in parallel, *i.e.* knowledge of the unfavorable effect of the *para*-CF₃ group on the benzyl ring on protein–ligand affinity was not yet available. It can be assumed with great confidence that similar ligands without the

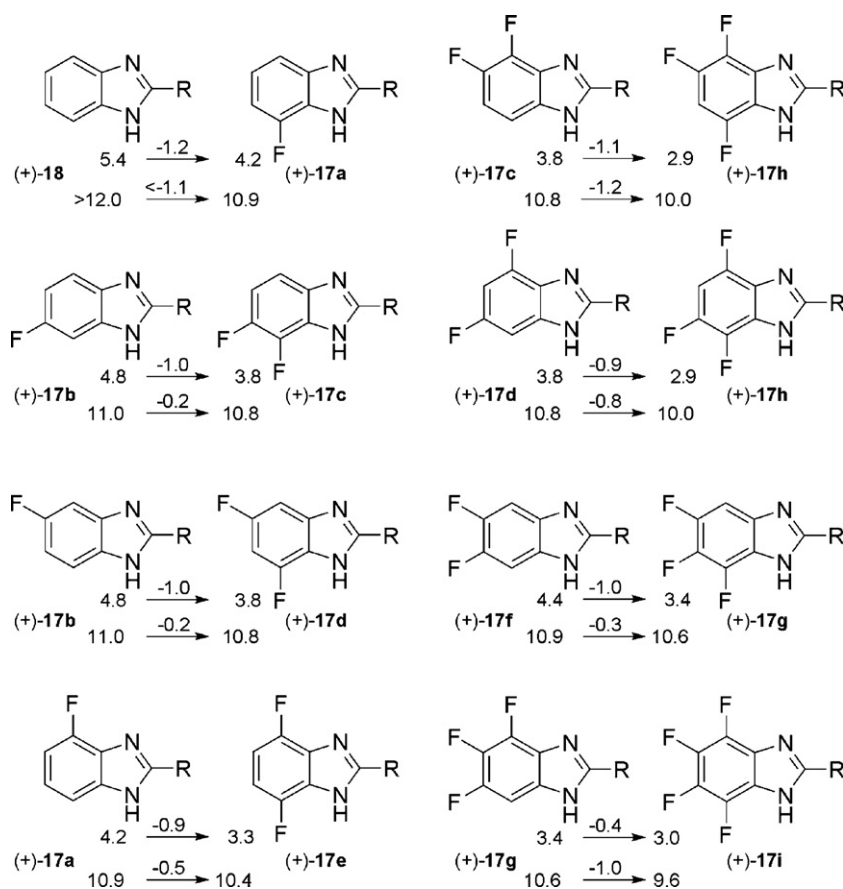


Fig. 4. ΔpK_a effects observed upon introduction of a fluorine substituent in *ortho*-position to a nitrogen atom in substituted benzimidazoles. R = $-\text{CH}(\text{CH}_2\text{OH})-\text{CH}_2-\text{C}_6\text{H}_4-p\text{-CF}_3$. Accuracy of pK_a measurements: ± 0.1 units.

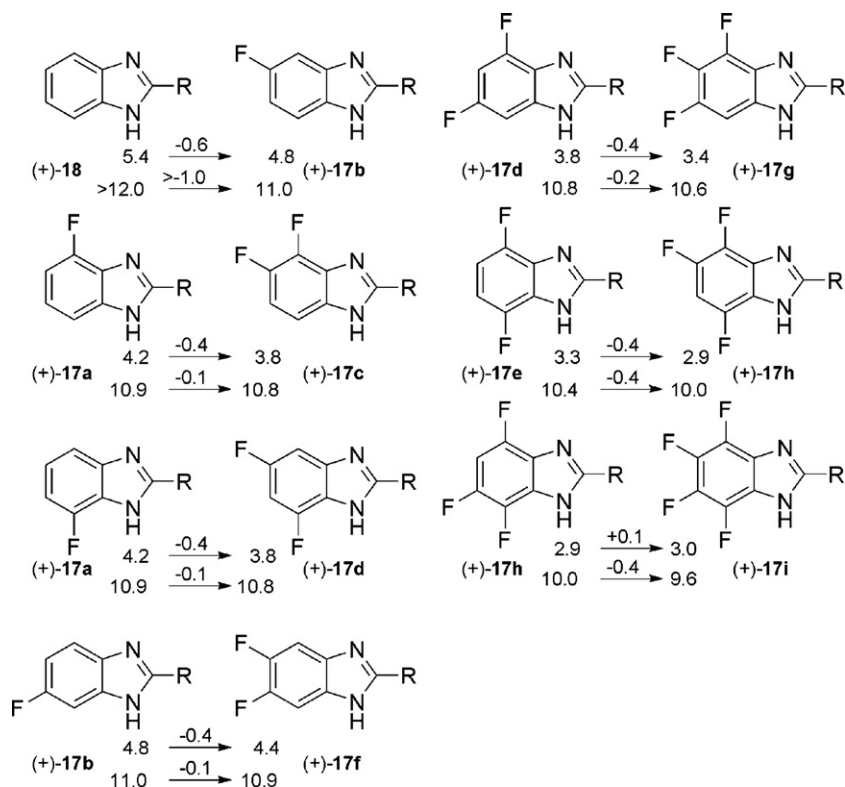


Fig. 5. ΔpK_{a1} effects observed upon introduction of a fluorine substituent in *meta*-position to a nitrogen atom in substituted benzimidazoles. $R = -CH(CH_2OH)-CH_2-C_6H_4-p-CF_3$. Accuracy of pK_a measurements: ± 0.1 units.

CF_3 group would have affinities in the lower nanomolar range. Nevertheless, interesting hints on favorable interactions of C–F residues with Arg side chains were obtained and they provided the starting point for subsequent database mining in the Protein Databank (PDB) to conclusively show that these side chains provide a fluorophilic environment [30].

Organic fluorine clearly encounters a more favorable protein environment around the central platform than in the S1' pocket. While fluorination of the benzyl ring to fill the S1' pocket increased the IC_{50} values from 9 nM ((+)-**1a** to 160–430 nM (+)-**5a–j**, Table 1), H/F substitution of the benzimidazole maintained most of the binding potency or even increased it as shown by the comparison between (+)-**3b** (520 nM) and (+)-**16a–i** (170–950 nM) (Table 2). The F-substituents in (+)-**16a–i** can affect binding affinity both through favorable/unfavorable interactions with the protein and by altering the pK_a values of the imidazole moiety [47], which were also measured (Table 2).

Since all IC_{50} values are within an order of magnitude, strong conclusions cannot be drawn. Nevertheless, roughly speaking, F-substituents in *ortho*-position to the imidazole ring lead to low affinity ((+)-**16a**, (+)-**16e**, (+)-**16h**, IC_{50} values: 500–1000 nM). The pK_a values of the imidazole N-atoms are lowered (see below), and this could lead to a weakened H-bond between the imidazole N-atom and the side chain of Arg717. Furthermore, molecular modeling, as shown in Fig. 3 for the tetrafluoro derivative (+)-**16i**, indicates that *ortho*-F-atoms undergo unfavorable interactions with the side chains of Phe106 and Trp693 (shortest distances $F \cdots C_{arom}$ of 3.2 and 3.1 Å, respectively). These two unfavorable effects seem to become compensated by electrostatically favorable interactions of the C–F bonds with the side chains of Arg110 and Arg717.

The introduction of F-atoms in *meta*-position is more favorable: binding potency increases from 520 nM ((+)-**3b**, no F) to 310 nM ((+)-**16b**, 1 *meta*-F), and to 170 nM ((+)-**16f**, 2 *meta*-F). The modeling suggests that the two *meta*-F-atoms interact favorably with the side

chain of Arg102 pointing orthogonally into the positively charged guanidinium residue. The reduction of the pK_{a1} value is weaker upon *meta*- than *ortho*-F-substitution and the H-bond between the imidazole N-atom and the side chain of Arg717 will not be weakened as much. Clearly, any loss in H-bonding efficiency is overcompensated by the additional C–F \cdots Arg102 interactions.

Following these findings, we performed a search in the PDB for C–F interactions with the guanidinium group of arginine residues and observed a high number of such interactions, which according to available structure–activity relationships add to protein–ligand binding affinities [30]. Rather than undergoing linear C–F \cdots H–N interactions, which is in agreement with the inefficiency of poorly polarizable organic fluorine to undergo H-bonding interactions [48], C–F bonds preferentially orient either parallel or more orthogonally to the guanidinium plane with its delocalized positive charge. The latter orientation is supported by the modeling for the C–F_{meta} \cdots Arg102 interaction in the complexes of NEP. The model shown in Fig. 3 is obtained starting from the crystal structure of (+)-**1a** complexed to NEP (PDB code 1Y8J) by substituting the pyridine ring by an annulated tetrafluorobenzene ring, followed by energy-minimization of the ligand while keeping the protein fixed, except for the flexible side chain of Arg102.

2.4. Trends in pK_a values of fluorinated benzimidazoles

Benzimidazoles are common scaffolds in medicinal chemistry and therefore it was of interest to investigate fluorine effects on their pK_a values. Table 2 gives the pK_a values for the protonation (pK_{a1}) and deprotonation (pK_{a2}) of precursor compounds to (+)-**3b** and (+)-**16a–i** in which the thiomethyl (CH_2SH) residue is exchanged for hydroxymethyl (CH_2OH). We refer to them in the following as (+)-**18** and (+)-**17a–i**. This change enables cleaner determination of the pK_{a1} and pK_{a2} values without interference of an additional ionization step by thiol deprotonation.

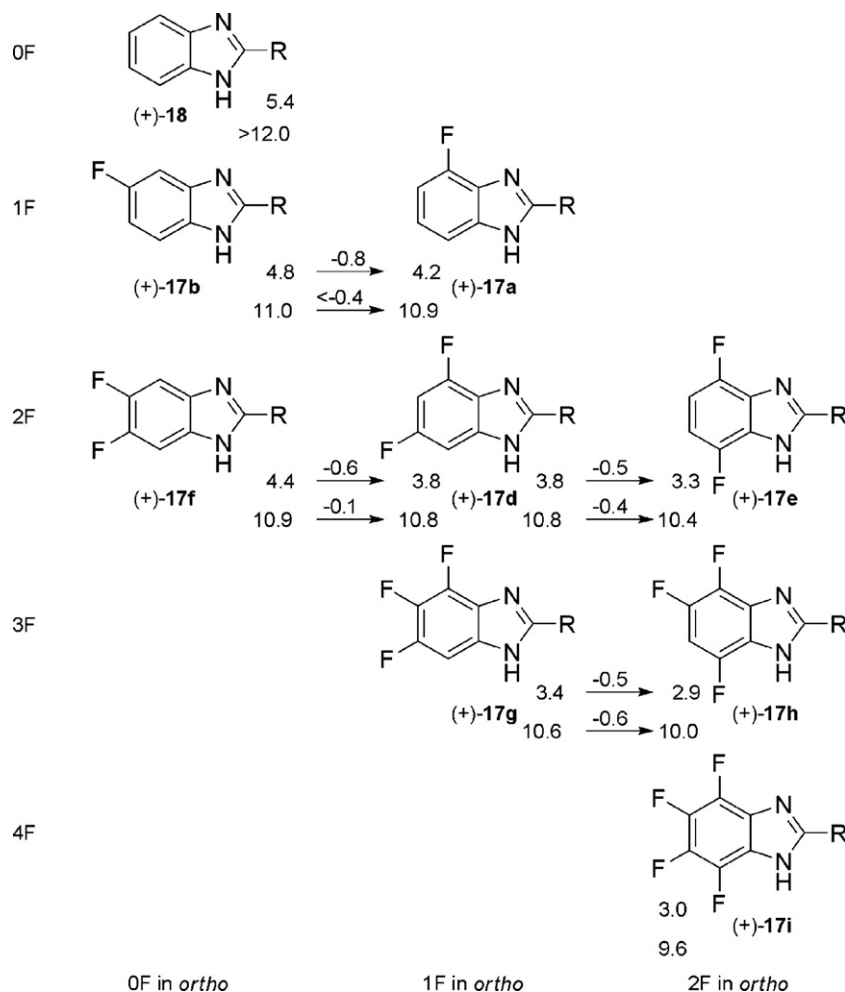


Fig. 6. ΔpK_{a1} effects observed for the shift of a fluorine substituent from a *meta*- to *ortho*-position to a nitrogen atom in substituted benzimidazoles. R = $-\text{CH}(\text{CH}_2\text{OH})-\text{CH}_2-\text{C}_6\text{H}_4-\text{p}-\text{CF}_3$. Accuracy of pK_a measurements: ± 0.1 units.

Interesting correlations between the pK_a values and the degree of fluorination at the benzene ring were observed. They are explicitly shown in Figs. 4–6. Note that for non-symmetrical cases such as (+)-17a, two different values for each pK_{a1} and pK_{a2} would have to be considered in principle if tautomerization were slow relative to pK_a measurements. However, we have no experimental evidence for “split” pK_a values.

Upon initial inspection of the data, increasing fluorination of the phenyl ring strongly affects both pK_a values, as expected, which shift in the case of pK_{a1} from 5.4 ((+)-18) to 3.0 ((+)-17i), and in the case of pK_{a2} from >12 ((+)-18) to 9.6 ((+)-17i) (Table 2). At equal degrees of fluorination, remarkable variation in the pK_a values is observed which corroborates the importance of the position of the F-atoms. Introduction of fluorine *ortho* to an N-atom in the benzimidazole system has a larger effect than *meta*-substitution. Thus, *ortho*-derivative (+)-17a features a pK_{a1} value of 4.2, whereas for *meta*-derivative (+)-17b, a value of 4.8 is measured. Similarly, in the difluorinated series, (+)-17e with two *ortho*-fluorines features pK_a 3.3, whereas the value for bis-*meta*-substituted (+)-17f is 1.1 units higher (4.4).

A more detailed analysis of the data shows remarkably consistent correlations. When comparing pairs of compounds that differ only by one additional fluorine at the *ortho*-position to an imidazole nitrogen, a decrease in pK_{a1} of 1.1 ± 0.2 units is observed, independent of the number of fluorine atoms in the starting compound (Fig. 4).

Similarly, introduction of an additional fluorine in the *meta*-position decreases the pK_{a1} values by 0.5 ± 0.1 units for all pairs of compounds (Fig. 5).

Shifting a fluorine from *meta* to *ortho* leads to a decrease of 0.6 ± 0.2 units for each series of mono- to tri-fluorinated benzimidazoles, again corroborating the weaker effect of *meta*-fluorination (Fig. 6). Similar, but less consistent patterns are observed for pK_{a2} values (Figs. 4–6).

The only compound not fitting the pattern is tetrafluorinated (+)-17i with an experimental pK_{a1} value of 3.0, which is 0.1 units higher than the tri-fluorinated derivative (+)-17h (2.9). According to the pattern derived in Fig. 4, this compound should have pK_{a1} of ca. 2.3 (introducing an *ortho*-fluorine into (+)-17g). When using the pattern of Fig. 5, a pK_{a1} of ca. 2.4 can be calculated (introducing a *meta*-fluorine into (+)-17h). At this point, we do not have a good explanation for the special acid/base properties of tetrafluorinated (+)-17i. Overall, the trends of pK_a shifts upon F-introduction in (+)-17a–i are in good agreement with those reported for simple fluorinated benzimidazoles [47].

3. Conclusions

While the introduction of organic fluorine into drugs and agrochemicals has for decades been a popular and successful approach to optimize physical (pK_a , $\log D$) and ADME (adsorption, distribution, metabolism, and excretion) properties, recent

research explores how binding potency and selectivity can be gained by direct interactions of C–F bonds in bound ligands with the surrounding protein environment. This study confirms the observed trend, that organic fluorine, with its high negative charge density and its low polarizability, prefers to orientate into electropositive protein environments [30]. Thus introduction of fluorine into the benzyl ring, used by our ligands to fill the S1' pocket, leads to substantial losses in binding potency. This narrow pocket is lined by several aromatic rings, and high-confidence modeling suggests that electronegative F-substituents closely approach their electron-rich π -surfaces. The resulting electrostatic repulsion makes the S1' pocket a highly fluorophobic environment. Of course, there are many reports in medicinal chemistry on filling hydrophobic cavities with CF_3 and other fluorinated residues. Partitioning becomes more favorable (positive $\log D$), desolvation entropy is gained, and C–H...F contacts are established, which all should enhance the measurable binding affinity. However, these gains in affinity can become compensated by losses in affinity resulting from close, electrostatically repulsive contacts between organic fluorine, with its high negative charge density, and the negatively polarized π -clouds of the side chains of Phe, Tyr, and Trp. We had previously also observed the fluorophobicity of the electron-rich indole ring of a Trp residue in our fluorine scan of thrombin inhibitors [25].

In contrast, binding potency is maintained or even increased, when the central benzimidazole platform of the ligands is fluorinated. Here, the highly reproducible modeling suggests that C–F bonds point orthogonally on the positively charged guanidinium side chains of surrounding Arg residues. The resulting electrostatically favorable interaction is quite general, as was shown in subsequent database searches [30]. Finally, pK_a measurement of the fluorinated ligands provided several simple patterns for the prediction of pK_a values of benzimidazoles, important building blocks in medicinal chemistry.

4. Experimental

4.1. General

Characterization. Melting points were obtained with a Büchi B-540 and are uncorrected. IR spectra were obtained with a PerkinElmer Spectrum BX FTIR Spectrometer from the neat substances. NMR spectra were recorded on Varian Gemini 300, Varian Mercury 300, or Bruker ARX 300 spectrometers. Chemical shifts in ^1H and ^{13}C NMR spectra are recorded as parts per million (ppm) referenced to the residual solvent resonances ($\text{CDCl}_3 = 7.26$, $\text{CH}_3\text{OD} = 3.31$). ^{19}F NMR spectra are recorded against CFCl_3 as internal standard ($\text{CFCl}_3 = 0$). Coupling constants are given in Hertz. High-resolution mass spectra were recorded on VG-TRIBRID (EI) or IonSpec Ultima (MALDI) spectrometers. 2,5-Dihydroxybenzoic acid (DHB) or 3-hydroxypicolinic acid (3-HPA) were used as matrix for MALDI-MS measurements. Elemental analyses were performed in the Laboratory of Organic Chemistry, ETH Zurich. Optical rotations were measured at 25 °C on a PerkinElmer 241 Polarimeter at 589 nm (Na-D line). The concentration c is given in g/100 mL. RP-HPLC was performed with Knauer ProntoSil columns (analytical: 120–5 C18 AQ, 250 mm \times 5.0 μm ; preparative: 120–5 C18 AQ, 250 mm \times 20 mm). The nomenclature follows suggestions of the computer program ACD/Name from ACD/Labs.

4.2. Enzyme assay

The affinities of inhibitors towards NEP were measured in a FRET-assay performed on a BMG Labtechnologies FLUOstar Optima

in 96 well-plates. Each inhibitor was prepared as a 4 mM stock solution in DMSO which was used to prepare 12 diluted solutions per inhibitor with concentrations between 100 and 0.001 μM in DMSO. Each well was loaded with 155 μL of aqueous buffer solution (50 mM 4-(2-hydroxyethyl)-1-piperazineethanesulfonic acid (HEPES), 100 mM NaCl, 0.2% of a 5% bovine serum albumin (BSA) solution in water, pH 7.4), 5 μL of the respective inhibitor solution in DMSO, 20 μL of 18.75 nM NEP solution in aqueous buffer (25 mM 2-amino-2-(hydroxymethyl)propane-1,3-diol (Tris), 200 mM NaCl, 2 mM MgCl_2 , pH 8.0), and 20 μL of substrate in buffer solution (0.8% solution of substrate Abz-GGfLRRVQ-EDDnp in MeOH, diluted to 62.5 μM with aqueous buffer solution (50 mM HEPES, 100 mM NaCl, containing 0.2% of a 5% BSA solution in water, pH 7.4)). Cleavage of the substrate was measured without preincubation of the prepared mixtures at $\lambda_{\text{exc}} = 320$ nm and $\lambda_{\text{em}} = 410$ nm. The affinity of each inhibitor was determined by two measurements per concentration. The determination of the respective IC_{50} value was performed in Microsoft Excel. The percentage of inhibition was determined by comparing the averaged slopes of the fluorescence lines to a reference value of a measurement containing no inhibitor.

The reproducibility of the IC_{50} values is $\pm 10\%$. Thiorphan as reference ligand gave an IC_{50} value of 6.0 ± 0.3 ($n = 4$) in this assay ([18]: 4 nM).

4.3. Molecular modeling

All modeling was done on a PC using the modeling package MOLOC for Windows and the all atom force field MAB [20]. All simulations started from the crystal structure of (+)-**1a** complexed to NEP (PDB code 1Y8J). The pyridine ring or the benzyl ring of (+)-**1a** were substituted by the newly introduced residues, and the new bound ligands were energy-minimized. The protein coordinates were kept fixed, except for the flexible side chain of Arg102. The modeling shown in Figs. 2 and 3 is highly reproducible when repeated by other co-workers in the laboratory.

4.4. Experimental procedures

All inhibitors were synthesized in identical reaction sequences, with minor improvements to those already described with full experimental protocols in Ref. [29]. A detailed synthesis of inhibitor (+)-**3a** is given in the following. Spectroscopic data only is given for all other inhibitors. Full experimental protocols can be found in a doctoral dissertation [49].

4.4.1. (+)-(4S)-4-Isopropyl-3-{3-[4-(trifluoromethyl)phenyl]propanoyl}-1,3-oxazolidin-2-one ((+)-**8**)

A solution of **6** (8.36 g, 38.3 mmol, 1.1 equiv.) in THF (190 mL) was cooled to -30 °C. Et_3N (12.6 mL, 90.6 mmol, 2.6 equiv.) and pivaloyl chloride (3.13 mL, 36.6 mmol, 1.05 equiv.) were added, and the suspension was stirred for 90 min. After addition of LiCl (1.70 g, 40.1 mmol, 1.15 equiv.) and oxazolidinone (S)-**7** (4.50 g, 34.8 mmol, 1.0 equiv.), the mixture was allowed to reach r.t. and stirred for 18 h. H_2O was added and the aqueous layer extracted with EtOAc. The combined organic layers were dried over MgSO_4 , concentrated, and the residue was purified by column chromatography (CC) (SiO_2 , pentane/EtOAc 7:1).

Yield: 7.77 g, 23.6 mmol, 68%. White solid. mp: 59 °C. $[\alpha]_{\text{D}}^{25}$: +53.8 ($c = 1.00$, CHCl_3). IR (neat): 2966, 1777, 1703, 1618, 1484, 1384, 1325, 1301, 1210, 1170, 1135, 1103, 1065, 1021, 998, 868, 831, 772, 750, 707. ^1H NMR (300 MHz, CDCl_3): 0.82 (d, $J = 6.9$, 3H), 0.90 (d, $J = 7.1$, 3H), 2.28–2.38 (m, 1H), 3.02–3.07 (m, 2H), 3.17–3.41 (m, 2H), 4.18–4.28 (m, 2H), 4.39–4.44 (m, 1H), 7.36/7.54 (AA'BB', $J = 8.3$, 4H). ^{13}C NMR (75 MHz, CDCl_3): 14.6, 18.0, 28.4,

30.2, 36.7, 58.4, 63.4, 124.1 (q, $J = 271.3$), 125.2 (q, $J = 3.6$), 128.4 (q, $J = 32.2$), 128.8, 144.5, 153.9, 171.7. ^{19}F NMR (282 MHz, CDCl_3): -62.8 (s, 3F). EI-HRMS: 329.1234 ($[\text{M}]^+$, $\text{C}_{16}\text{H}_{18}\text{F}_3\text{NO}_3^+$, calcd. 329.1233). Anal. calcd for $\text{C}_{16}\text{H}_{18}\text{F}_3\text{NO}_3$: C 58.36, H 5.51, N 4.25. Found: C 58.27, H 5.55, N 4.30.

4.4.2. (+)-(4S)-3-((2R)-3-(Benzyloxy)-2-[4-(trifluoromethyl)benzyl]propanoyl]-4-isopropyl-1,3-oxazolidin-2-one ((+)-9)

A solution of (+)-**8** (7.69 g, 23.3 mmol, 1.0 equiv.) in CH_2Cl_2 (115 mL) was cooled to 0°C , mixed with TiCl_4 (4.82 mL, 24.5 mmol, 1.05 equiv.), and stirred for 5 min. Diisopropylethylamine (3.30 mL, 23.3 mmol, 1.0 equiv.) was added, and stirring was continued for 1 h before BOMCl (6.50 mL, 46.7 mmol, 2.0 equiv.) was added. Stirring was continued for 3 h, then saturated aqueous NH_4Cl solution was added, and the aqueous layer was extracted with CH_2Cl_2 . The combined organic layers were dried over MgSO_4 and concentrated. The residue was purified by CC (SiO_2 , pentane/EtOAc 9:2).

Yield: 5.79 g, 12.9 mmol, 55%. Colorless oil. $[\alpha]_{\text{D}}^{25}$: $+43.5$ ($c = 1.12$, CHCl_3). IR (neat): 2963, 2873, 1771, 1699, 1617, 1453, 1385, 1362, 1322, 1300, 1202, 1161, 1114, 1065, 1017, 990, 846, 823, 735, 697. ^1H NMR (300 MHz, CDCl_3): 0.79 (d, $J = 6.9$, 3H), 0.87 (d, $J = 6.9$, 3H), 2.26–2.36 (m, 1H), 2.90 (dd, $J = 7.2$, 13.6, 1H), 3.08 (dd, $J = 8.1$, 13.6, 1H), 3.65 (dd, $J = 4.8$, 9.3, 1H), 3.76 (dd, $J = 6.8$, 9.3, 1H), 4.05–4.16 (m, 2H), 4.35–4.40 (m, 1H), 4.45–4.56 (m, 3H), 7.25–7.37 (m, 7H), 7.51 (d, $J = 8.3$, 2H). ^{13}C NMR (75 MHz, CDCl_3): 14.6, 17.9, 28.4, 34.4, 45.2, 58.4, 63.2, 70.5, 73.1, 124.1 (q, $J = 271.3$), 125.1 (q, $J = 3.5$), 127.5, 128.1, 128.5 (q, $J = 32.2$), 129.3, 137.7, 142.8, 153.5, 173.2. ^{19}F NMR (282 MHz, CDCl_3): -62.7 (s, 3F). MALDI-HRMS (3-HPA): 472.1703 ($[\text{MNa}]^+$, $\text{C}_{24}\text{H}_{26}\text{F}_3\text{NO}_4\text{Na}^+$, calcd 472.1706). Anal. calcd for $\text{C}_{24}\text{H}_{26}\text{F}_3\text{NO}_4$: C 64.13, H 5.83, N 3.12. Found: C 64.01, H 5.75, N 3.15.

4.4.3. (+)-(4S)-3-((2R)-3-Hydroxy-2-[4-(trifluoromethyl)benzyl]propanoyl]-4-isopropyl-1,3-oxazolidin-2-one ((+)-10)

To a solution of (+)-**9** (5.36 g, 11.9 mmol, 1.0 equiv.) in EtOAc (100 mL), Pd/C (10% Pd, 1.27 g, 0.1 equiv.) was added and the mixture was stirred under an atmosphere of H_2 for 24 h. Filtration through Celite and concentration of the solution gave crude product which was purified by CC (SiO_2 , pentane/EtOAc 2:1).

Yield: 3.89 g, 10.8 mmol, 91%. White solid. mp: 108°C . $[\alpha]_{\text{D}}^{25}$: $+93.7$ ($c = 1.01$, CHCl_3). IR (neat): 3475, 2962, 2940, 2877, 1747, 1700, 1616, 1483, 1418, 1399, 1373, 1325, 1303, 1291, 1221, 1161, 1124, 1109, 1063, 1018, 982, 942, 861, 829, 777, 759, 705, 641. ^1H NMR (300 MHz, CDCl_3): 0.87 (d, $J = 6.9$, 3H), 0.90 (d, $J = 7.0$, 3H), 2.29–2.42 (m, 1H), 2.45 (dd, $J = 4.2$, 8.1, 1H), 2.90 (dd, $J = 7.6$, 13.4, 1H), 3.07 (dd, $J = 7.6$, 13.4, 1H), 3.74 (ddd, $J = 6.7$, 8.1, 11.1, 1H), 3.86 (td, $J = 4.2$, 11.1, 1H), 4.09–4.20 (m, 2H), 4.25–4.37 (m, 2H), 7.37/7.52 (AA'BB', $J = 8.0$, 4H). ^{13}C NMR (75 MHz, CDCl_3): 14.6, 17.8, 28.4, 33.9, 46.9, 58.7, 63.1, 63.5, 124.2 (q, $J = 271.8$), 125.3 (q, $J = 3.7$), 128.8 (q, $J = 32.2$), 129.5, 142.7, 154.0, 174.5. ^{19}F NMR (282 MHz, CDCl_3): -62.2 (s, 3F). MALDI-HRMS (3-HPA): 382.1236 ($[\text{MNa}]^+$, $\text{C}_{17}\text{H}_{20}\text{F}_3\text{NO}_4\text{Na}^+$, calcd 382.1237). Anal. calcd for $\text{C}_{17}\text{H}_{20}\text{F}_3\text{NO}_4$: C 56.82, H 5.61, N 3.90. Found: C 56.59, H 5.66, N 3.84.

4.4.4. (+)-(4S)-3-((2R)-3-[[tert-Butyl(dimethyl)silyloxy]-2-[4-(trifluoromethyl)benzyl]propanoyl]-4-isopropyl-1,3-oxazolidin-2-one ((+)-11)

To a solution of (+)-**10** (1.00 g, 2.78 mmol, 1.0 equiv.) in CH_2Cl_2 (3.5 mL), TBDMSCl (0.629 g, 4.17 mmol, 1.5 equiv.) and DMAp (0.578 g, 4.73 mmol, 1.7 equiv.) were added. After stirring for 18 h, the mixture was diluted with H_2O and CH_2Cl_2 and the aqueous layer was extracted with CH_2Cl_2 . The combined organic layers

were dried over MgSO_4 and concentrated. The residue was purified by CC (SiO_2 , pentane/EtOAc 8:1).

Yield: 1.31 g, 2.77 mmol, 99%. White solid. mp: 61°C . $[\alpha]_{\text{D}}^{25}$: $+61.7$ ($c = 0.99$, MeOH). IR (neat): 2952, 2930, 2883, 2857, 1764, 1701, 1617, 1465, 1387, 1371, 1323, 1301, 1259, 1243, 1228, 1216, 1162, 1110, 1092, 1067, 1018, 963, 939, 836, 823, 777, 724, 697, 682, 666, 636. ^1H NMR (300 MHz, CDCl_3): 0.01 (s, 3H), 0.02 (s, 3H), 0.84 (d, $J = 6.9$, 3H), 0.86 (s, 9H), 0.88 (d, $J = 7.1$, 3H), 2.22–2.37 (m, 1H), 2.87 (dd, $J = 6.9$, 13.6, 1H), 3.03 (dd, $J = 8.3$, 13.6, 1H), 3.80 (dd, $J = 4.6$, 9.8, 1H), 3.90 (dd, $J = 6.4$, 9.8, 1H), 4.08–4.15 (m, 2H), 4.31–4.40 (m, 2H), 7.33/7.51 (AA'BB', $J = 8.2$, 4H). ^{13}C NMR (75 MHz, CDCl_3): -5.61 , -5.55 , 14.8, 17.9, 18.2, 25.8, 28.5, 34.2, 47.4, 58.4, 63.2, 63.7, 124.2 (q, $J = 271.8$), 125.3 (q, $J = 3.7$), 128.4 (q, $J = 32.4$), 129.5, 143.2, 153.7, 173.3. ^{19}F NMR (282 MHz, CDCl_3): -62.8 (s, 3F). MALDI-HRMS (3-HPA): 496.2091 ($[\text{MNa}]^+$, $\text{C}_{23}\text{H}_{34}\text{F}_3\text{NO}_4\text{NaSi}^+$, calcd 496.2101). Anal. calcd for $\text{C}_{23}\text{H}_{34}\text{F}_3\text{NO}_4\text{Si}$: C 58.33, H 7.24, N 2.96. Found: C 58.27, H 7.30, N 2.91.

4.4.5. (–)-(2R)-3-[[tert-Butyl(dimethyl)silyloxy]-2-[4-(trifluoromethyl)benzyl]propanoic acid ((–)-12)

To a degassed solution of (+)-**11** (2.81 g, 5.93 mmol, 1.0 equiv.) in THF (80 mL) and H_2O (25 mL), H_2O_2 (30% in H_2O , 4.04 mL, 35.6 mmol, 6.0 equiv.) and a degassed solution of $\text{LiOH}\cdot\text{H}_2\text{O}$ (0.498 g, 11.9 mmol, 2.0 equiv.) in H_2O (12 mL) were added at 0°C . The mixture was stirred for 3 h at 0°C , then 16 h at r.t. A solution of aqueous Na_2SO_3 (1.5 M, 35 mL) was added, stirring was continued for 15 min, then THF was removed *in vacuo*. The residue was diluted with Et_2O , and aqueous HCl solution (1 M) was added until a pH value of 1–2 was reached. The mixture was then quickly extracted with Et_2O , the organic layer dried over MgSO_4 and concentrated. The residue was purified by flash chromatography (SiO_2 , pentane/EtOAc 10:1, with 0.5% AcOH added).

Yield: 1.46 g, 4.04 mmol, 90%. White solid. mp: 41°C . $[\alpha]_{\text{D}}^{25}$: -1.54 ($c = 1.01$, CHCl_3). IR (neat): 2926, 2855, 1706, 1619, 1469, 1460, 1419, 1360, 1321, 1252, 1218, 1159, 1107, 1087, 1065, 1035, 1018, 1004, 976, 952, 939, 866, 832, 815, 805, 771, 731, 676. ^1H NMR (300 MHz, CDCl_3): 0.04 (s, 3H), 0.04 (s, 3H), 0.89 (s, 9H), 2.81–2.90 (m, 1H), 2.95 (dd, $J = 6.9$, 13.7, 1H), 3.06 (dd, $J = 7.6$, 13.7, 1H), 3.74 (dd, $J = 5.9$, 10.0, 1H), 3.80 (dd, $J = 5.1$, 10.0, 1H), 7.32/7.54 (AA'BB', $J = 8.0$, 4H). ^{13}C NMR (75 MHz, CDCl_3): -5.42 , 18.3, 25.8, 33.5, 49.3, 62.6, 124.1 (q, $J = 271.3$), 125.3 (q, $J = 3.6$), 128.7 (q, $J = 32.2$), 129.2, 142.8, 178.4. ^{19}F NMR (282 MHz, CDCl_3): -62.2 (s, 3F). EI-HRMS: 305.0816 ($[\text{M}-\text{C}_4\text{H}_9]^+$, $\text{C}_{13}\text{H}_{16}\text{F}_3\text{O}_3\text{Si}^+$, calcd 305.0815). Anal. calcd for $\text{C}_{17}\text{H}_{25}\text{F}_3\text{O}_3\text{Si}$: C 56.33, H 6.95. Found: C 56.05, H 6.95.

4.4.6. (+)-(2R)-N-(3-Amino-4-pyridinyl)-3-[[tert-butyl(dimethyl)silyloxy]-2-[4-(trifluoromethyl)benzyl]propanamide ((+)-13)

To a 0°C cold solution of (–)-**12** (0.300 g, 0.828 mmol, 1.0 equiv.) in CH_2Cl_2 (8.3 mL), oxalylchloride (2 M solution in CH_2Cl_2 , 0.44 mL, 0.869 mmol, 1.05 equiv.) was added and the mixture stirred at r.t. for 12 h. The solvent was removed *in vacuo* and the residue redissolved in THF (8.3 mL). After addition of 3,4-diaminopyridine (0.181 g, 1.66 mmol, 2.0 equiv.) and Et_3N (0.23 mL, 1.66 mmol, 2.0 equiv.), the mixture was stirred for 12 h. H_2O was added and THF removed *in vacuo*. The aqueous layer was extracted with CH_2Cl_2 and the organic layer dried over MgSO_4 . The concentrated residue was then purified by CC (SiO_2 , EtOAc).

Yield: 0.357 g, 0.787 mmol, 95%. White solid. mp: 161°C . $[\alpha]_{\text{D}}^{25}$: $+11.0$ ($c = 0.55$, CHCl_3). IR (neat): 3163, 2950, 2929, 2857, 1698, 1682, 1617, 1579, 1532, 1470, 1427, 1387, 1323, 1296, 1247, 1196, 1186, 1166, 1105, 1064, 1017, 1004, 835, 822, 776, 733, 667. ^1H NMR (300 MHz, CDCl_3): 0.06 (s, 3H), 0.07 (s, 3H), 0.89 (s, 9H), 2.79–2.89 (m, 2H), 3.11–3.20 (m, 1H), 3.63 (s br., 2H), 3.83 (d, $J = 5.3$, 2H),

7.23 (d, $J = 5.2$, 1H), 7.33/7.55 (AA'BB', $J = 8.0$, 4H), 7.97 (d, $J = 5.3$, 1H), 8.07 (s, 1H), 8.49 (s br., 1H). ^{13}C NMR (75 MHz, CDCl_3): -5.38 , -5.34 , 18.3, 25.9, 34.4, 51.4, 64.0, 117.0, 124.0 (q, $J = 271.3$), 125.4 (q, $J = 3.5$), 128.8 (q, $J = 32.3$), 129.2, 131.9, 134.6, 140.4, 141.3, 142.9, 171.9. ^{19}F NMR (282 MHz, CDCl_3): -62.2 (s, 3F). MALDI-HRMS (3-HPA): 454.2126 ($[\text{MH}]^+$, $\text{C}_{22}\text{H}_{30}\text{F}_3\text{N}_3\text{O}_2\text{Si}^+$, calcd 454.2132). Anal. calcd for $\text{C}_{22}\text{H}_{30}\text{F}_3\text{N}_3\text{O}_2\text{Si}$: C 58.26, H 6.67, N 9.26. Found: C 58.48, H 6.91, N 9.27.

4.4.7. (+)-(2S)-2-(1H-Imidazo[4,5-c]pyridin-2-yl)-3-[4-(trifluoromethyl)phenyl]-1-propanol ((+)-14)

A solution of (+)-**13** (0.258 g, 0.569 mmol, 1.0 equiv.) in AcOH (40 mL) was warmed to 65°C for 24 h. The solvent was removed *in vacuo*, and traces of AcOH were removed by azeotropic distillation with toluene. The residue was redissolved in THF (2.3 mL) and *n*Bu₄NF (2 M solution in THF, 0.57 mL, 1.14 mmol, 2.0 equiv.) was added. After stirring for 2 h, the THF was removed *in vacuo*. The residue was mixed with H₂O and extracted with EtOAc. The combined organic layers were dried over MgSO₄ and concentrated. The residue was purified by CC (SiO₂, EtOAc/MeOH 9:1).

Yield: 0.112 g, 0.349 mmol, 61%. White solid. mp: 83°C . $[\alpha]_{\text{D}}^{25}$: $+94.8$ ($c = 0.22$, CHCl_3). IR (neat): 3084, 2936, 1620, 1591, 1533, 1460, 1419, 1322, 1285, 1159, 1107, 1065, 1031, 1018, 970, 913, 848, 812, 630. ^1H NMR (300 MHz, $\text{CDCl}_3 + 3$ drops of TFA): 3.13–3.24 (m, 2H), 3.51–3.60 (m, 1H), 3.83 (dd, $J = 7.0$, 11.0, 1H), 3.90 (dd, $J = 5.2$, 11.0, 1H), 7.21/7.38 (AA'BB', $J = 8.0$, 4H), 7.89 (dd, $J = 0.7$, 6.5, 1H), 8.26 (dd, $J = 0.7$, 6.5, 1H), 8.95 (s, 1H). ^{13}C NMR (75 MHz, $\text{CDCl}_3 + 3$ drops of TFA): 35.6, 44.7, 63.2, 111.9, 123.9 (q, $J = 276.4$), 125.3 (q, $J = 3.5$), 128.8 (q, $J = 32.6$), 129.0, 130.6, 132.2, 137.0, 142.2, 147.7, 165.9. ^{19}F NMR (282 MHz, $\text{CDCl}_3 + 3$ drops of TFA): -62.7 (s, 3F). MALDI-HRMS (3-HPA): 322.1155 ($[\text{MH}]^+$, $\text{C}_{16}\text{H}_{15}\text{F}_3\text{N}_3\text{O}^+$, calcd 322.1162).

4.4.8. (–)-S-((2S)-2-(1H-imidazo[4,5-c]pyridin-2-yl)-3-[4-(trifluoromethyl)phenyl]propyl) ethanethioate ((–)-15)

To a 0°C cold solution of PPh₃ (0.123 g, 0.468 mmol, 1.5 equiv.) in THF (4.7 mL), DIAD (0.093 mL, 0.468 mmol, 1.5 equiv.) was added and the mixture stirred for 30 min. A solution of (+)-**14** (0.100 g, 0.311 mmol, 1.0 equiv.) in THF (3.1 mL) and AcSH (0.044 mL, 0.624 mmol, 2.0 equiv.) were subsequently added. The mixture was stirred at 0°C for 1 h and at r.t. for 2 h, then H₂O was added. The aqueous layer was extracted with Et₂O, the combined organic layers were dried over MgSO₄ and concentrated. The residue was purified by CC (SiO₂, EtOAc/MeOH 95:5).

Yield: 0.089 g, 0.235 mmol, 75%. White solid. mp: 67°C . $[\alpha]_{\text{D}}^{25}$: -78.4 ($c = 0.23$, MeOH). IR (neat): 3069, 2998, 2965, 2874, 1774, 1702, 1600, 1545, 1509, 1482, 1453, 1406, 1389, 1370, 1318, 1305, 1209, 1157, 1142, 1123, 1101, 1064, 1050, 1019, 999, 971, 864, 827, 787, 749, 733, 696, 637. ^1H NMR (300 MHz, $\text{CDCl}_3 + 3$ drops of TFA): 2.28 (s, 3H), 3.29–3.41 (m, 2H), 3.50 (dd, $J = 5.2$, 14.1, 1H), 3.58 (t, $J = 14.1$, 1H), 3.79–3.87 (m, 1H), 7.24/7.43 (AA'BB', $J = 8.1$, 4H), 8.05 (d, $J = 6.5$, 1H), 8.32 (d, $J = 6.5$, 1H), 9.25 (s, 1H). ^{13}C NMR (75 MHz, $\text{CDCl}_3 + 3$ drops of TFA): 30.5, 32.2, 39.4, 42.6, 113.8, 123.9 (q, $J = 271.1$), 125.4 (q, $J = 3.4$), 129.0, 129.0 (q, $J = 32.4$), 130.0, 132.2, 135.1, 141.1, 149.4, 166.1, 194.7. ^{19}F NMR (282 MHz, $\text{CDCl}_3 + 3$ drops of TFA): -62.3 (s, 3F). MALDI-HRMS (3-HPA): 380.1031 ($[\text{MH}]^+$, $\text{C}_{18}\text{H}_{17}\text{F}_3\text{N}_3\text{OS}^+$, calcd 380.1039).

4.4.9. (+)-(2S)-2-(1H-Imidazo[4,5-c]pyridin-2-yl)-3-[4-(trifluoromethyl)phenyl]-1-propanethiol trifluoroacetate ((+)-3a)

A solution of (–)-**15** (0.067 g, 0.177 mmol, 1.0 equiv.) in MeOH (3.5 mL) was first degassed with Ar, then with H₂, and a degassed solution of NaOMe (0.5 M solution in MeOH, 3.54 mL, 1.77 mmol, 10.0 equiv.) was added. The solution was stirred for 2 h, then the solvent was removed *in vacuo*. The residue was diluted with H₂O

and CH_2Cl_2 and quickly extracted with CH_2Cl_2 . The combined organic layers were dried over MgSO₄ and concentrated. The residue was dissolved in a 1:1 mixture of MeCN/H₂O (3 mL), filtered through cotton wool, and immediately purified by preparative RP-HPLC (gradient 0.1% TFA in H₂O/MeCN 99:1 → 0:100 in 60 min). The fractions containing the product as TFA salt were combined and lyophilized.

Yield: 0.039 g, 0.086 mmol, 49%. Colorless oil. $[\alpha]_{\text{D}}^{25}$: $+44.6$ ($c = 0.11$, MeOH). IR (neat): 3060, 3029, 2996, 2967, 2955, 2870, 1770, 1703, 1603, 1489, 1482, 1453, 1406, 1389, 1379, 1368, 1362, 1306, 1226, 1210, 1141, 1122, 1102, 1066, 1021, 997, 970, 915, 787, 771, 709, 700, 639. ^1H NMR (300 MHz, CDCl_3): 2.88–3.10 (m, 3H), 3.16–3.24 (m, 1H), 3.38–3.44 (m, 1H), 7.18–7.25 (m, 2H), 7.37 (d, $J = 6.4$, 1H), 7.73–7.83 (m, 2H), 8.22 (d, $J = 6.4$, 1H), 9.34 (s, 1H). ^{13}C NMR (75 MHz, CDCl_3): 33.5, 37.5, 43.1, 105.2, 124.1 (q, $J = 268.5$), 126.5, 129.4 (q, $J = 3.4$), 130.9 (q, $J = 32.8$), 133.1, 134.8, 137.2, 142.7, 146.8, 158.2. ^{19}F NMR (282 MHz, CDCl_3): -62.5 (s, 3F). MALDI-HRMS (DHB): 338.0930 ($[\text{MH}]^+$, $\text{C}_{16}\text{H}_{15}\text{F}_3\text{N}_3\text{S}^+$, calcd 338.0933).

4.4.10. (+)-(2S)-2-(1H-Benzimidazol-2-yl)-3-[4-(trifluoromethyl)phenyl]-1-propanethiol trifluoroacetate ((+)-3b)

Colorless oil. $[\alpha]_{\text{D}}^{25}$: $+49.7$ ($c = 0.13$, MeOH). IR (neat): 3239, 2929, 2857, 1652, 1620, 1527, 1499, 1461, 1415, 1389, 1362, 1320, 1247, 1165, 1112, 1066, 1017, 905, 831, 783, 739, 667, 628. ^1H NMR (300 MHz, CD_3OD): 2.91–3.07 (m, 3H), 3.13–3.19 (m, 1H), 3.42–3.48 (m, 1H), 7.20–7.24 (m, 2H), 7.27–7.32 (m, 2H), 7.73–7.80 (m, 4H). ^{13}C NMR (75 MHz, CDCl_3): 33.5, 37.5, 43.1, 114.0, 124.1 (q, $J = 266.3$), 127.5, 129.5 (q, $J = 3.6$), 130.2 (q, $J = 32.2$), 131.8, 137.0, 142.7, 156.9. ^{19}F NMR (282 MHz, CDCl_3): -62.3 (s, 3F). MALDI-HRMS (DHB): 337.0984 ($[\text{MH}]^+$, $\text{C}_{17}\text{H}_{16}\text{F}_3\text{N}_2\text{S}^+$, calcd 337.0981).

4.4.11. (+)-(2S)-2-(1H-Imidazo[4,5-c]pyridin-2-yl)-3-[4-methylphenyl]-1-propanethiol trifluoroacetate ((+)-4a)

Colorless oil. $[\alpha]_{\text{D}}^{25}$: $+48.5$ ($c = 0.09$, CHCl_3). IR (neat): 3048, 2922, 1639, 1620, 1596, 1539, 1500, 1450, 1426, 1327, 1237, 1190, 1153, 1109, 1067, 1045, 1018, 872, 954, 935, 848, 820, 783, 742, 658. ^1H NMR (300 MHz, CD_3OD): 2.20 (s, 3H), 3.12–3.26 (m, 4H), 3.54–3.63 (m, 1H), 6.89–7.00 (m, 4H), 8.00–8.04 (m, 1H), 8.47–8.50 (m, 1H), 9.14–9.17 (m, 1H). ^{13}C NMR (75 MHz, CD_3OD): 21.0, 28.3, 40.5, 43.8, 112.0, 114.7, 118.5, 129.8, 130.3, 133.4, 136.3, 137.7, 139.8, 166.9. MALDI-HRMS (3-HPA): 284.1212 ($[\text{MH}]^+$, $\text{C}_{16}\text{H}_{18}\text{N}_3\text{S}^+$, calcd 284.1216).

4.4.12. (+)-(2S)-3-(4-Cyclobutylphenyl)-2-(1H-imidazo[4,5-c]pyridin-2-yl)-1-propanethiol trifluoroacetate ((+)-4b)

Colorless oil. $[\alpha]_{\text{D}}^{25}$: $+54.7$ ($c = 0.12$, CHCl_3). IR (neat): 3072, 2734, 1698, 1616, 1538, 1489, 1454, 1445, 1425, 1324, 1270, 1190, 1165, 1122, 1107, 1065, 1030, 1016, 958, 851, 828, 766, 751, 731, 617. ^1H NMR (300 MHz, CD_3OD): 1.75–1.84 (m, 1H), 1.92–2.10 (m, 3H), 2.20–2.31 (m, 2H), 3.02–3.28 (m, 4H), 3.36–3.47 (m, 1H), 6.96–7.05 (m, 4H), 8.03 (d, $J = 7.0$, 1H), 8.49 (d, $J = 7.0$, 1H), 9.17 (s, 1H). ^{13}C NMR (75 MHz, CD_3OD): 19.0, 28.3, 30.8, 40.4, 40.5, 41.4, 112.1, 127.5, 129.7, 133.3, 134.4, 136.7, 139.8, 145.9, 147.9, 167.4. MALDI-HRMS (3-HPA): 324.1530 ($[\text{MH}]^+$, $\text{C}_{19}\text{H}_{21}\text{N}_3\text{S}^+$, calcd 324.1529).

4.4.13. (+)-(2S)-3-(4-Cyclopentylphenyl)-2-(1H-imidazo[4,5-c]pyridin-2-yl)-1-propanethiol trifluoroacetate ((+)-4c)

Colorless oil. $[\alpha]_{\text{D}}^{25}$: $+46.1$ ($c = 0.11$, CHCl_3). IR (neat): 3468, 2935, 1747, 1698, 1481, 1397, 1361, 1298, 1215, 1141, 1125, 1103, 1077, 1054, 985, 944, 847, 820, 773, 754, 700, 638. ^1H NMR (300 MHz, CD_3OD): 1.31–2.09 (m, 8H), 2.81–3.07 (m, 4H), 3.50–3.80 (m, 2H), 6.92–7.06 (m, 4H), 8.01 (d, $J = 6.3$, 1H), 8.47 (d, $J = 6.3$, 1H), 9.14 (s, 1H). ^{13}C NMR (75 MHz, CD_3OD): 26.4, 35.7, 40.5, 41.1, 43.7, 46.9, 112.2, 128.4, 129.8, 133.4, 134.5, 136.3, 139.8, 146.4,

147.9, 167.0. MALDI-HRMS (3-HPA): 338.1686 ([MH]⁺, C₂₀H₂₄N₃S⁺, calcd 338.1684).

4.4.14. (+)-(2S)-3-(4-Cyclohexylphenyl)-2-(1H-imidazo[4,5-c]pyridin-2-yl)-1-propanethiol trifluoroacetate ((+)-4d)

Colorless oil. [α]_D²⁵: +44.8 (c = 0.07, CHCl₃). IR (neat): 3056, 3002, 2967, 2877, 1773, 1700, 1608, 1515, 1484, 1464, 1451, 1435, 1406, 1389, 1372, 1312, 1280, 1206, 1143, 1116, 1102, 1063, 1049, 1019, 997, 970, 947, 892, 881, 821, 789, 766, 749, 730, 697, 644, 616. ¹H NMR (300 MHz, CD₃OD): 1.23–1.44 (m, 5H), 1.68–1.87 (m, 5H), 2.35–2.46 (m, 1H), 3.03–3.27 (m, 4H), 3.54–3.63 (m, 1H), 6.92–7.04 (m, 4H), 8.03 (d, J = 6.7, 1H), 8.49 (d, J = 6.7, 1H), 9.17 (s, 1H). ¹³C NMR (75 MHz, CD₃OD): 27.2, 28.0, 28.3, 35.7, 40.4, 45.6, 48.4, 112.1, 128.1, 128.1, 129.8, 133.3, 134.4, 136.7, 139.8, 147.9, 167.4. MALDI-HRMS (3-HPA): 352.1842 ([MH]⁺, C₂₁H₂₆N₃S⁺, calcd 352.1842).

4.4.15. (+)-(2S)-3-(4-Fluorophenyl)-2-(1H-imidazo[4,5-c]pyridin-2-yl)-1-propanethiol trifluoroacetate ((+)-5a)

Colorless oil. [α]_D²⁵: +41.7 (c = 0.08, CHCl₃). IR (neat): 3468, 2935, 1747, 1698, 1481, 1397, 1361, 1298, 1215, 1141, 1125, 1103, 1077, 1054, 985, 944, 847, 820, 773, 754, 700, 638. ¹H NMR (300 MHz, CD₃OD): 3.12–3.28 (m, 4H), 3.77–3.87 (m, 1H), 6.87–6.93 (m, 2H), 7.03–7.08 (m, 2H), 8.01 (dd, J = 0.7, 6.7, 1H), 8.49 (dd, J = 0.7, 6.7, 1H), 9.16 (t, J = 0.7, 1H). ¹³C NMR (75 MHz, CD₃OD): 31.1, 35.2, 40.4, 112.2, 116.4 (d, J = 21.5), 131.7 (d, J = 8.0), 133.6, 134.6, 135.1 (d, J = 3.3), 139.8, 147.8, 163.2 (d, J = 242.8), 166.6. ¹⁹F NMR (282 MHz, CD₃OD): –116.8 (m, 1F). MALDI-HRMS (3-HPA): 288.0960 ([MH]⁺, C₁₅H₁₅FN₃S⁺, calcd 288.0965).

4.4.16. (+)-(2S)-3-(3-Fluorophenyl)-2-(1H-imidazo[4,5-c]pyridin-2-yl)-1-propanethiol trifluoroacetate ((+)-5b)

Colorless oil. [α]_D²⁵: +52.9 (c = 0.09, CHCl₃). IR (neat): 3065, 3030, 2967, 2939, 2870, 2793, 1759, 1702, 1593, 1497, 1474, 1452, 1427, 1400, 1382, 1359, 1298, 1249, 1200, 1125, 1103, 1091, 1054, 1043, 1029, 1013, 983, 945, 882, 825, 772, 737, 711, 692, 621. ¹H NMR (300 MHz, CD₃OD): 3.14–3.27 (m, 4H), 3.80–3.90 (m, 1H), 6.81–6.91 (m, 3H), 7.14–7.22 (m, 1H), 8.02 (dd, J = 0.8, 6.6, 1H), 8.49 (dd, J = 0.8, 6.6, 1H), 9.17 (t, J = 0.8, 1H). ¹³C NMR (75 MHz, CD₃OD): 31.1, 37.1, 40.4, 112.2, 114.8 (d, J = 2.8), 116.6 (d, J = 21.4), 125.8 (d, J = 2.7), 131.5 (d, J = 8.5), 133.6, 134.6, 139.7, 141.9 (d, J = 7.7), 147.8, 164.3 (d, J = 245.6), 166.5. ¹⁹F NMR (282 MHz, CD₃OD): –113.8 (m, 1F). MALDI-HRMS (3-HPA): 288.0963 ([MH]⁺, C₁₅H₁₅FN₃S⁺, calcd 288.0965).

4.4.17. (+)-(2S)-3-(2-Fluorophenyl)-2-(1H-imidazo[4,5-c]pyridin-2-yl)-1-propanethiol trifluoroacetate ((+)-5c)

Colorless Oil. [α]_D²⁵: +58.3 (c = 0.12, CHCl₃). IR (neat): 3048, 2922, 1639, 1620, 1596, 1539, 1500, 1450, 1426, 1327, 1237, 1190, 1153, 1109, 1067, 1045, 1018, 872, 954, 935, 848, 820, 783, 742, 658. ¹H NMR (300 MHz, CD₃OD): 3.15–3.28 (m, 4H), 3.82–3.92 (m, 1H), 6.93–7.07 (m, 3H), 7.15–7.23 (m, 1H), 8.01 (dd, J = 0.8, 6.6, 1H), 8.49 (dd, J = 0.8, 6.6, 1H), 9.15 (t, J = 0.8, 1H). ¹³C NMR (75 MHz, CD₃OD): 29.8, 31.1, 38.0, 112.1, 116.4 (d, J = 22.0), 125.5 (d, J = 3.4), 125.8 (d, J = 15.6), 130.2 (d, J = 8.3), 132.4 (d, J = 4.4), 133.6, 134.6, 139.9, 147.8, 162.5 (d, J = 247.3), 166.4. ¹⁹F NMR (282 MHz, CD₃OD): –118.8 (m, 1F). MALDI-HRMS (3-HPA): 288.0961 ([MH]⁺, C₁₅H₁₅FN₃S⁺, calcd 288.0965).

4.4.18. (+)-(2S)-3-(3,4-Difluorophenyl)-2-(1H-imidazo[4,5-c]pyridin-2-yl)-1-propanethiol trifluoroacetate ((+)-5d)

Colorless oil. [α]_D²⁵: +57.8 (c = 0.12, CHCl₃). IR (neat): 3484, 3389, 3236, 2933, 2860, 1686, 1661, 1638, 1532, 1487, 1442, 1417, 1390, 1363, 1321, 1257, 1233, 1214, 1165, 1105, 1066, 1044, 1031, 1018, 1006, 954, 910, 851, 833, 753, 671, 628. ¹H NMR (300 MHz, CD₃OD): 3.13–3.27 (m, 4H), 3.79–3.89 (m, 1H), 6.80–6.86 (m, 1H),

6.96–7.09 (m, 2H), 8.03 (dd, J = 0.7, 6.6, 1H), 8.49 (dd, J = 0.7, 6.6, 1H), 9.17 (t, J = 0.7, 1H). ¹³C NMR (75 MHz, CD₃OD): 31.1, 37.1, 40.4, 112.2, 118.4 (d, J = 17.2), 118.8 (d, J = 17.3), 126.4 (dd, J = 3.6, 6.2), 133.6, 134.6, 136.7 (t, J = 4.8), 139.8, 147.9, 150.5 (dd, J = 12.6, 246.0), 151.4 (dd, J = 12.9, 247.1), 166.3. ¹⁹F NMR (282 MHz, CD₃OD): –139.0 (m, 1F), –142.0 (m, 1F). MALDI-HRMS (3-HPA): 304.0870 ([MH]⁺, C₁₅H₁₄F₂N₃S⁺, calcd 304.0871).

4.4.19. (+)-(2S)-3-(2,4-Difluorophenyl)-2-(1H-imidazo[4,5-c]pyridin-2-yl)-1-propanethiol trifluoroacetate ((+)-5e)

Colorless oil. [α]_D²⁵: +49.8 (c = 0.11, CHCl₃). IR (neat): 3031, 2964, 2927, 2860, 1764, 1703, 1616, 1583, 1493, 1483, 1457, 1397, 1382, 1358, 1296, 1274, 1246, 1228, 1219, 1201, 1173, 1141, 1124, 1104, 1089, 1052, 1028, 1012, 982, 960, 943, 909, 894, 845, 807, 778, 760, 738, 730, 692, 625, 611. ¹H NMR (300 MHz, CD₃OD): 3.08 (d, J = 7.1, 2H), 3.20 (dd, J = 8.9, 13.6, 1H), 3.35 (dd, J = 6.6, 13.6, 1H), 3.59–3.68 (m, 1H), 6.74–6.88 (m, 2H), 7.13 (dt, J = 6.5, 8.6, 1H), 8.06 (dd, J = 0.8, 6.6, 1H), 8.51 (dd, J = 0.8, 6.6, 1H), 9.19 (t, J = 0.8, 1H). ¹³C NMR (75 MHz, CD₃OD): 28.2, 33.6, 46.8, 104.7 (t, J = 26.1), 112.1, 112.4 (dd, J = 3.7, 21.4), 122.2 (dd, J = 3.8, 15.9), 133.4, 134.5, 139.9, 147.9, 162.5 (dd, J = 12.0, 247.0), 163.5 (dd, J = 12.2, 246.8), 166.7. ¹⁹F NMR (282 MHz, CD₃OD): –112.5 (m, 1F), –114.3 (dd, J = 8.6, 17.4, 1F). MALDI-HRMS (3-HPA): 306.0864 ([MH]⁺, C₁₅H₁₄F₂N₃S⁺, calcd 306.0871).

4.4.20. (+)-(2S)-3-(2,3-Difluorophenyl)-2-(1H-imidazo[4,5-c]pyridin-2-yl)-1-propanethiol trifluoroacetate ((+)-5f)

Colorless oil. [α]_D²⁵: +47.1 (c = 0.07, CHCl₃). IR (neat): 3072, 2734, 1698, 1616, 1538, 1489, 1454, 1445, 1425, 1324, 1270, 1190, 1165, 1122, 1107, 1065, 1030, 1016, 958, 851, 828, 766, 751, 731, 617. ¹H NMR (300 MHz, CD₃OD): 3.09 (d, J = 7.2, 2H), 3.23–3.28 (m, 1H), 3.39–3.46 (m, 1H), 3.62–3.72 (m, 1H), 6.88–7.00 (m, 2H), 7.07 (dtd, J = 1.9, 8.0, 10.1, 1H), 8.06 (dd, J = 0.7, 6.6, 1H), 8.51 (dd, J = 0.7, 6.6, 1H), 9.19 (t, J = 0.7, 1H). ¹³C NMR (75 MHz, CD₃OD): 28.3, 33.8, 46.7, 112.1, 117.1 (d, J = 17.3), 125.6 (dd, J = 4.8, 6.9), 127.2 (t, J = 3.3), 128.8 (d, J = 12.3), 133.6, 134.5, 139.9, 147.8, 150.3 (dd, J = 12.9, 245.7), 151.9 (dd, J = 13.1, 246.8), 166.5. ¹⁹F NMR (282 MHz, CD₃OD): –139.7 (m, 1F), –144.5 (td, J = 6.8, 20.6, 1F). MALDI-HRMS (3-HPA): 304.0871 ([MH]⁺, C₁₅H₁₄F₂N₃S⁺, calcd 304.0871).

4.4.21. (+)-(2S)-3-(2,5-Difluorophenyl)-2-(1H-imidazo[4,5-c]pyridin-2-yl)-1-propanethiol trifluoroacetate ((+)-5g)

Colorless oil. [α]_D²⁵: +61.7 (c = 0.11, CHCl₃). IR (neat): 3069, 2998, 2965, 2874, 1774, 1702, 1600, 1545, 1509, 1482, 1453, 1406, 1389, 1370, 1318, 1305, 1209, 1157, 1142, 1123, 1101, 1064, 1050, 1019, 999, 971, 864, 827, 787, 749, 733, 696, 637. ¹H NMR (300 MHz, CD₃OD): 3.16–3.29 (m, 4H); 3.84–3.94 (m, 1H), 6.83–7.04 (m, 3H), 8.03 (dd, J = 0.8, 6.6, 1H), 8.50 (dd, J = 0.8, 6.6, 1H), 9.17 (t, J = 0.8, 1H). ¹³C NMR (75 MHz, CD₃OD): 31.1, 31.6, 38.0, 112.1, 116.4 (dd, J = 8.5, 24.6), 117.7 (dd, J = 9.4, 26.0), 118.5 (dd, J = 5.2, 18.3), 127.6 (dd, J = 6.1, 16.4), 133.7, 134.6, 139.9, 147.8, 162.0 (dd, J = 2.7, 248.1), 162.7 (dd, J = 2.7, 249.6), 166.0. ¹⁹F NMR (282 MHz, CD₃OD): –119.5 (m, 1F), –124.5 (m, 1F). MALDI-HRMS (3-HPA): 304.0874 ([MH]⁺, C₁₅H₁₄F₂N₃S⁺, calcd 304.0871).

4.4.22. (+)-(2S)-3-(2,6-Difluorophenyl)-2-(1H-imidazo[4,5-c]pyridin-2-yl)-1-propanethiol trifluoroacetate ((+)-5h)

Colorless oil. [α]_D²⁵: +40.6 (c = 0.08, CHCl₃). IR (neat): 3450, 2941, 1682, 1601, 1572, 1500, 1386, 1306, 1169, 1083, 1013, 980, 820, 771, 675, 628. ¹H NMR (300 MHz, CD₃OD): 3.19–3.33 (m, 4H), 3.83–3.92 (m, 1H), 6.85 (t, J = 8.0, 2H), 7.19–7.29 (m, 1H), 8.03 (dd, J = 0.8, 6.6, 1H), 8.51 (dd, J = 0.8, 6.6, 1H), 9.15 (t, J = 0.8, 1H). ¹³C

NMR (75 MHz, CD₃OD): 27.8, 41.3, 41.8, 112.2 (d, *J* = 9.5), 112.6, 114.4 (t, *J* = 20.1), 130.6 (t, *J* = 10.5), 133.7, 134.7, 139.9, 147.9, 162.8 (dd, *J* = 8.1, 246.8), 166.0. ¹⁹F NMR (282 MHz, CD₃OD): –115.6 (t, *J* = 6.9, 2F). MALDI-HRMS (3-HPA): 304.0865 ([MH]⁺, C₁₅H₁₄F₂N₃S⁺, calcd 306.0871).

4.4.23. (+)-(2*S*)-3-(3,5-Difluorophenyl)-2-(1*H*-imidazo[4,5-*c*]pyridin-2-yl)-1-propanethiol trifluoroacetate ((+)-5*i*)

Colorless oil. [α]_D²⁵: +52.4 (*c* = 0.10, CHCl₃). IR (neat): 3056, 3002, 2967, 2877, 1773, 1700, 1608, 1515, 1484, 1464, 1451, 1435, 1406, 1389, 1372, 1312, 1280, 1206, 1143, 1116, 1102, 1063, 1049, 1019, 997, 970, 947, 892, 881, 821, 789, 766, 749, 730, 697, 644, 616. ¹H NMR (300 MHz, CD₃OD): 3.05–3.10 (m, 2H), 3.23 (dd, *J* = 9.3, 13.6, 1H), 3.10–3.37 (m, 1H), 3.60–3.70 (m, 1H), 6.68–6.79 (m, 3H), 8.06 (dd, *J* = 0.8, 6.6, 1H), 8.50 (dd, *J* = 0.8, 6.6, 1H), 9.20 (t, *J* = 0.8, 1H). ¹³C NMR (75 MHz, CD₃OD): 28.5, 40.0, 47.6, 103.0 (t, *J* = 25.7), 112.2, 112.9 (dd, *J* = 7.8, 17.1), 133.6, 134.5, 139.9, 144.0 (t, *J* = 9.2), 147.8, 164.5 (dd, *J* = 13.1, 247.5), 166.5. ¹⁹F NMR (282 MHz, CD₃OD): –110.6 (m, 2F). MALDI-HRMS (3-HPA): 304.0867 ([MH]⁺, C₁₅H₁₄F₂N₃S⁺, calcd 304.0871).

4.4.24. (+)-(2*S*)-2-(1*H*-Imidazo[4,5-*c*]pyridin-2-yl)-3-(pentafluorophenyl)-1-propanethiol trifluoroacetate ((+)-5*j*)

Colorless oil. [α]_D²⁵: +48.7 (*c* = 0.11, CHCl₃). IR (neat): 3049, 2921, 1620, 1592, 1537, 1445, 1419, 1364, 1325, 1273, 1189, 1164, 1109, 1067, 1018, 986, 972, 939, 903, 849, 805, 767, 739, 619. ¹H NMR (300 MHz, CD₃OD): 3.26–3.44 (m, 4H), 3.83–3.91 (m, 1H), 8.07 (dd, *J* = 0.7, 6.5, 1H), 8.52 (dd, *J* = 0.7, 6.5, 1H), 9.19 (t, *J* = 0.7, 1H). ¹³C NMR (75 MHz, CD₃OD): 27.6, 41.5, 48.2, 112.3, 115.4/117.9 (mm), 119.2 (m), 133.9, 134.7, 137.2/140.5 (mm), 139.9, 145.1/148.3 (mm), 147.9, 165.2. ¹⁹F NMR (282 MHz, CD₃OD): –143.8 (dd, *J* = 8.0, 21.6, 2F), –157.6 (t, *J* = 20.0, 1F), –157.6 (m, 2F). MALDI-HRMS (3-HPA): 358.0587 ([MH]⁺, C₁₅H₁₁F₅N₃S⁺, calcd 360.0588).

4.4.25. (+)-(2*S*)-2-(7-Fluoro-1*H*-benzimidazol-2-yl)-3-[4-(trifluoromethyl)phenyl]-1-propanethiol trifluoroacetate ((+)-16*a*)

Colorless oil. [α]_D²⁵: +63.8 (*c* = 0.13, CHCl₃). IR (neat): 3484, 3389, 3236, 2933, 2860, 1686, 1661, 1638, 1532, 1487, 1442, 1417, 1390, 1363, 1321, 1257, 1233, 1214, 1165, 1105, 1066, 1044, 1031, 1018, 1006, 954, 910, 851, 833, 753, 671, 628. ¹H NMR (300 MHz, CD₃OD): 3.06 (dd, *J* = 9.3, 14.1, 1H), 3.18 (dd, *J* = 5.6, 14.1, 1H), 3.30 (dd, *J* = 9.3, 13.7, 1H), 3.48 (dd, *J* = 6.4, 13.7, 1H), 3.85 (tt, *J* = 5.6, 9.3, 1H), 7.28–7.31 (m, 1H), 7.35/7.53 (AA'BB', *J* = 8.3, 4H), 7.48–7.58 (m, 2H). ¹³C NMR (75 MHz, CD₃OD): 27.8, 39.6, 46.7, 111.2 (d, *J* = 4.5), 112.6 (d, *J* = 16.2), 121.9 (d, *J* = 16.9), 125.4 (q, *J* = 250.6), 126.8 (q, *J* = 3.6), 128.4 (d, *J* = 6.5), 130.5, 130.6 (q, *J* = 32.4), 135.3 (d, *J* = 3.6), 142.9, 150.7 (d, *J* = 250.9), 156.8. ¹⁹F NMR (282 MHz, CD₃OD): –62.9 (s, 3F), –129.6 (dd, *J* = 4.5, 10.6, 1F). MALDI-HRMS (3-HPA): 355.0893 ([MH]⁺, C₁₇H₁₅F₄N₂S⁺, calcd 355.0887).

4.4.26. (+)-(2*S*)-2-(6-Fluoro-1*H*-benzimidazol-2-yl)-3-[4-(trifluoromethyl)phenyl]-1-propanethiol trifluoroacetate ((+)-16*b*)

Colorless oil. [α]_D²⁵: +64.7 (*c* = 0.13, CHCl₃). IR (neat): 3450, 2941, 1682, 1601, 1572, 1500, 1386, 1306, 1169, 1083, 1013, 980, 820, 771, 675, 628. ¹H NMR (300 MHz, CD₃OD): 3.03 (dd, *J* = 9.3, 14.1, 1H), 3.19 (dd, *J* = 5.6, 14.1, 1H), 3.28 (dd, *J* = 9.5, 13.9, 1H), 3.47 (dd, *J* = 6.3, 13.9, 1H), 3.79–3.89 (m, 1H), 7.34/7.55 (AA'BB', *J* = 8.0, 4H), 7.34–7.41 (m, 1H), 7.51–7.56 (m, 1H), 7.75 (ddd, *J* = 0.5, 4.3, 9.1, 1H). ¹³C NMR (75 MHz, CD₃OD): 27.7, 39.5, 46.6, 101.7 (d, *J* = 28.5), 116.3 (d, *J* = 24.0), 116.6 (d, *J* = 7.8), 125.5 (q, *J* = 271.1), 126.9 (q, *J* = 3.7), 130.5, 130.7 (q, *J* = 32.6), 132.9 (d, *J* = 13.5), 142.9, 156.8 (d, *J* = 1.3), 162.6 (d, *J* = 244.7), 164.2. ¹⁹F NMR (282 MHz, CD₃OD): –63.0 (s, 3F), –114.1 (m, 1F).

MALDI-HRMS (3-HPA): 355.0889 ([MH]⁺, C₁₇H₁₅F₄N₂S⁺, calcd 355.0887).

4.4.27. (+)-(2*S*)-2-(6,7-Difluoro-1*H*-benzimidazol-2-yl)-3-[4-(trifluoromethyl)phenyl]-1-propanethiol trifluoroacetate ((+)-16*c*)

Colorless oil. [α]_D²⁵: +61.3 (*c* = 0.12, CHCl₃). IR (neat): 3049, 2921, 1620, 1592, 1537, 1445, 1419, 1364, 1325, 1273, 1189, 1164, 1109, 1067, 1018, 986, 972, 939, 903, 849, 805, 767, 739, 619. ¹H NMR (300 MHz, CD₃OD): 3.04 (dd, *J* = 9.0, 14.0, 1H), 3.12 (dd, *J* = 5.7, 14.0, 1H), 3.27 (dd, *J* = 9.4, 13.6, 1H), 3.43 (dd, *J* = 6.2, 13.6, 1H), 3.67–3.77 (m, 1H), 7.32/7.51 (AA'BB', *J* = 8.1, 4H), 7.35–7.46 (m, 2H). ¹³C NMR (75 MHz, CD₃OD): 28.1, 39.9, 47.1, 110.7 (d, *J* = 3.5), 115.8 (d, *J* = 16.7), 125.6 (q, *J* = 271.2), 125.9, 126.7 (q, *J* = 3.7), 130.4 (q, *J* = 32.2), 130.5, 132.6 (d, *J* = 4.9), 139.6 (dd, *J* = 16.1, 253.4), 143.4, 148.6 (dd, *J* = 9.4, 240.4), 158.5. ¹⁹F NMR (282 MHz, CD₃OD): –62.9 (s, 3F), –143.3 (m, 1F), –154.2 (m, 1F). MALDI-HRMS (3-HPA): 373.0791 ([MH]⁺, C₁₇H₁₄F₅N₂S⁺, calcd 373.0792).

4.4.28. (+)-(2*S*)-2-(5,7-Difluoro-1*H*-benzimidazol-2-yl)-3-[4-(trifluoromethyl)phenyl]-1-propanethiol trifluoroacetate ((+)-16*d*)

Colorless oil. [α]_D²⁵: +57.9 (*c* = 0.10, CHCl₃). IR (neat): 3065, 3030, 2967, 2939, 2870, 2793, 1759, 1702, 1593, 1497, 1474, 1452, 1427, 1400, 1382, 1359, 1298, 1249, 1200, 1125, 1103, 1091, 1054, 1043, 1029, 1013, 983, 945, 882, 825, 772, 737, 711, 692, 621. ¹H NMR (300 MHz, CD₃OD): 3.02 (dd, *J* = 9.0, 14.1, 1H), 3.15 (dd, *J* = 5.3, 14.1, 1H), 3.27 (dd, *J* = 9.3, 13.9, 1H), 3.46 (dd, *J* = 6.2, 13.9, 1H), 3.76 (ddt, *J* = 5.3, 6.2, 9.0, 1H), 7.25 (ddd, *J* = 2.1, 9.9, 10.5, 1H), 7.34/7.56 (AA'BB', *J* = 8.0, 4H), 7.33–7.37 (m, 1H). ¹³C NMR (75 MHz, CD₃OD): 27.9, 39.7, 47.0, 97.9 (dd, *J* = 4.2, 27.2), 102.5 (m), 122.4, 125.6 (q, *J* = 267.9), 126.9 (q, *J* = 3.8), 130.6, 130.6 (q, *J* = 33.1), 135.6, 143.1, 153.8 (dd, *J* = 6.3, 243.8), 157.9, 158.2 (dd, *J* = 5.8, 244.2). ¹⁹F NMR (282 MHz, CD₃OD): –62.9 (s, 3F), –116.5 (m, 1F), –126.7 (m, 1F). MALDI-HRMS (3-HPA): 373.0789 ([MH]⁺, C₁₇H₁₄F₅N₂S⁺, calcd 373.0792).

4.4.29. (+)-(2*S*)-2-(4,7-Difluoro-1*H*-benzimidazol-2-yl)-3-[4-(trifluoromethyl)phenyl]-1-propanethiol trifluoroacetate ((+)-16*e*)

Colorless oil. [α]_D²⁵: +47.1 (*c* = 0.09, CHCl₃). IR (neat): 3056, 3002, 2967, 2877, 1773, 1700, 1608, 1515, 1484, 1464, 1451, 1435, 1406, 1389, 1372, 1312, 1280, 1206, 1143, 1116, 1102, 1063, 1049, 1019, 997, 970, 947, 892, 881, 821, 789, 766, 749, 730, 697, 644, 616. ¹H NMR (300 MHz, CD₃OD): 3.04 (dd, *J* = 9.1, 14.0, 1H), 3.11 (dd, *J* = 6.0, 14.0, 1H), 3.26 (dd, *J* = 9.3, 13.8, 1H), 3.43 (dd, *J* = 6.4, 13.8, 1H), 3.62–3.72 (m, 1H), 7.17 (t, *J* = 6.5, 2H), 7.32/7.55 (AA'BB', *J* = 8.2, 4H). ¹³C NMR (75 MHz, CD₃OD): 28.2, 40.1, 47.4, 111.2 (m), 125.7 (q, *J* = 272.8), 126.8 (q, *J* = 3.5), 130.5 (q, *J* = 32.4), 130.6, 135.6, 143.5 (m), 147.6 (d, *J* = 250.4), 158.2. ¹⁹F NMR (282 MHz, CD₃OD): –62.8 (s, 3F), –135.8 (m, 2F). MALDI-HRMS (3-HPA): 373.0786 ([MH]⁺, C₁₇H₁₄F₅N₂S⁺, calcd 373.0792).

4.4.30. (+)-(2*S*)-2-(5,6-Difluoro-1*H*-benzimidazol-2-yl)-3-[4-(trifluoromethyl)phenyl]-1-propanethiol trifluoroacetate ((+)-16*f*)

Colorless oil. [α]_D²⁵: +45.7 (*c* = 0.09, CHCl₃). IR (neat): 3072, 2734, 1698, 1616, 1538, 1489, 1454, 1445, 1425, 1324, 1270, 1190, 1165, 1122, 1107, 1065, 1030, 1016, 958, 851, 828, 766, 751, 731, 617. ¹H NMR (300 MHz, CD₃OD): 3.03 (dd, *J* = 9.1, 14.1, 1H), 3.17 (dd, *J* = 5.3, 14.1, 1H), 3.28 (dd, *J* = 9.3, 13.8, 1H), 3.46 (dd, *J* = 6.3, 13.8, 1H), 3.79–3.89 (m, 1H), 7.34/7.54 (AA'BB', *J* = 8.1, 4H), 7.73 (t, *J* = 8.1, 2H). ¹³C NMR (75 MHz, CD₃OD): 27.8, 39.5, 46.6, 103.7 (dd, *J* = 9.4, 15.5), 125.5 (q, *J* = 271.2), 126.8 (q, *J* = 3.7), 128.3, 130.5, 130.6 (q, *J* = 32.4), 142.9, 151.3 (dd, *J* = 16.9, 249.4), 157.5. ¹⁹F NMR (282 MHz, CD₃OD): –62.9 (s, 3F), –139.2 (t, *J* = 8.1, 2F). MALDI-HRMS (3-HPA): 373.0782 ([MH]⁺, C₁₇H₁₄F₅N₂S⁺, calcd 373.0792).

4.4.31. (+)-(2S)-2-(5,6,7-Trifluoro-1H-benzimidazol-2-yl)-3-[4-(trifluoromethyl)phenyl]-1-propanethiol trifluoroacetate ((+)-16g)

Colorless oil. $[\alpha]_D^{25}$: +41.7 ($c = 0.09$, CHCl_3). IR (neat): 3056, 3002, 2967, 2877, 1773, 1700, 1608, 1515, 1484, 1464, 1451, 1435, 1406, 1389, 1372, 1312, 1280, 1206, 1143, 1116, 1102, 1063, 1049, 1019, 997, 970, 947, 892, 881, 821, 789, 766, 749, 730, 697, 644, 616. ^1H NMR (300 MHz, CD_3OD): 2.97–3.09 (m, 2H), 3.23 (dd, $J = 9.3$, 13.6, 1H), 3.37 (dd, $J = 6.1$, 13.6, 1H), 3.54–3.63 (m, 1H), 7.28/7.49 (AA'BB', $J = 8.1$, 4H), 7.32–7.36 (m, 1H). ^{13}C NMR (75 MHz, CD_3OD): 28.4, 40.2, 47.4, 97.9 (dd, $J = 4.1$, 23.3), 124.1 (m), 125.6 (q, $J = 271.1$), 126.6 (q, $J = 3.7$), 130.2 (q, $J = 32.3$), 130.5, 131.4 (m), 137.2/140.3 (mm), 139.3/142.6 (mm), 143.9, 148.8/152.1 (mm), 159.2. ^{19}F NMR (282 MHz, CD_3OD): –62.8 (s, 3F), –141.7 (dd, $J = 9.6$, 19.3, 1F), –152.5 (d, $J = 19.3$, 1F), –170.1 (dt, $J = 6.1$, 19.3, 1F). MALDI-HRMS (3-HPA): 391.0699 ($[\text{MH}]^+$, $\text{C}_{17}\text{H}_{13}\text{F}_6\text{N}_2\text{S}^+$, calcd 391.0698).

4.4.32. (+)-(2S)-2-(4,6,7-Trifluoro-1H-benzimidazol-2-yl)-3-[4-(trifluoromethyl)phenyl]-1-propanethiol trifluoroacetate ((+)-16h)

Colorless oil. $[\alpha]_D^{25}$: +49.7 ($c = 0.08$, CHCl_3). IR (neat): 3048, 2922, 1639, 1620, 1596, 1539, 1500, 1450, 1426, 1327, 1237, 1190, 1153, 1109, 1067, 1045, 1018, 872, 954, 935, 848, 820, 783, 742, 658. ^1H NMR (300 MHz, CD_3OD): 3.03 (d, $J = 7.2$, 2H), 3.22 (dd, $J = 9.4$, 13.5, 1H), 3.36 (dd, $J = 6.1$, 13.5, 1H), 3.47–3.57 (m, 1H), 7.07 (ddd, $J = 5.6$, 9.9, 11.4, 1H), 7.27/7.49 (AA'BB', $J = 8.0$, 4H). ^{13}C NMR (75 MHz, CD_3OD): 28.6, 40.5, 47.7, 100.2 (m), 114.9 (m), 118.7 (m), 125.0 (m), 125.7 (q, $J = 271.1$), 126.5 (q, $J = 4.0$), 130.1 (q, $J = 31.5$), 130.6, 135.2/138.3 (mm), 144.2, 145.0/148.3 (mm), 159.6. ^{19}F NMR (282 MHz, CD_3OD): –62.8 (s, 3F), –132.6 (dd, $J = 9.9$, 20.1, 1F), –145.6 (dd, $J = 11.5$, 19.8, 1F), –160.8 (dt, $J = 5.5$, 19.8, 1F). MALDI-HRMS (3-HPA): 391.0701 ($[\text{MH}]^+$, $\text{C}_{17}\text{H}_{13}\text{F}_6\text{N}_2\text{S}^+$, calcd 391.0698).

4.4.33. (+)-(2S)-2-(4,5,6,7-Tetrafluoro-1H-benzimidazol-2-yl)-3-[4-(trifluoromethyl)phenyl]-1-propanethiol trifluoroacetate ((+)-16i)

Colorless oil. $[\alpha]_D^{25}$: +40.7 ($c = 0.11$, CHCl_3). IR (neat): 3069, 2998, 2965, 2874, 1774, 1702, 1600, 1545, 1509, 1482, 1453, 1406, 1389, 1370, 1318, 1305, 1209, 1157, 1142, 1123, 1101, 1064, 1050, 1019, 999, 971, 864, 827, 787, 749, 733, 696, 637. ^1H NMR (300 MHz, CD_3OD): 3.01 (d, $J = 7.2$, 2H), 3.21 (dd, $J = 9.6$, 13.6, 1H), 3.34 (dd, $J = 6.1$, 13.6, 1H), 3.45–3.54 (m, 1H), 7.26/7.49 (AA'BB', $J = 8.0$, 4H). ^{13}C NMR (75 MHz, CD_3OD): 28.7, 40.6, 47.8, 124.6 (m), 125.7 (q, $J = 271.1$), 126.5 (q, $J = 3.5$), 130.1 (q, $J = 32.4$), 130.6, 135.3/138.6 (mm), 136.8/140.1 (mm), 144.3, 160.2. ^{19}F NMR (282 MHz, CD_3OD): –62.9 (s, 3F), –157.8 (m, 2F), –167.2 (m, 2F). MALDI-HRMS (3-HPA): 409.0608 ($[\text{MH}]^+$, $\text{C}_{17}\text{H}_{11}\text{F}_7\text{N}_2\text{S}^+$, calcd 409.0604).

Acknowledgements

This work was supported by the ETH research council and F. Hoffmann-La Roche, Basel.

References

- [1] A.J. Turner, K. Tanzawa, FASEB J. 11 (1997) 355–364.
- [2] N.D. Rawlings, D.P. Tolle, A.J. Barrett, Nucleic Acids Res. 32 (2004) D160–D164.
- [3] M.A. Kerr, A.J. Kenny, Biochem. J. 137 (1974) 477–488.
- [4] B.P. Roques, F. Noble, V. Daugé, M.-C. Fournié-Zaluski, A. Beaumont, Pharmacol. Rev. 45 (1993) 87–146.
- [5] B. Malfroy, J.P. Swerts, A. Guyon, B.P. Roques, J.C. Schwartz, Nature 276 (1978) 523–526.
- [6] R. Matsas, I.S. Fulcher, A.J. Kenny, A.J. Turner, Proc. Natl. Acad. Sci. U.S.A. 80 (1983) 3111–3115.
- [7] E.G. Erdős, R.A. Skidgel, FASEB J. 3 (1989) 145–151.
- [8] A.J. Kenny, S.L. Stephenson, FEBS Lett. 232 (1988) 1–8.
- [9] M.A. Shipp, G.E. Tarr, C.-Y. Chen, S.N. Switzer, L.B. Hersh, H. Stein, M.E. Sunday, E.L. Reinherz, Proc. Natl. Acad. Sci. U.S.A. 88 (1991) 10662–10666.
- [10] A.J. Turner, R.E. Isaac, D. Coates, BioEssays 23 (2001) 261–269.
- [11] N. Iwata, S. Tsubuki, Y. Takaki, K. Watanabe, M. Sekiguchi, E. Hosoki, M. Kawashima-Morishima, H.-J. Lee, E. Hama, J. Sekine-Aizawa, T.C. Saido, Nat. Med. 6 (2000) 143–150.
- [12] N. Iwata, S. Tsubuki, Y. Takaki, K. Shirohata, B. Lu, N.P. Gerard, C. Gerard, E. Hama, H.-J. Lee, T.C. Saido, Science 292 (2001) 1550–1552.
- [13] B.P. Roques, F. Noble, P. Crine, M.-C. Fournié-Zaluski, Methods Enzymol. 248 (1995) 263–283.
- [14] M.-C. Fournié-Zaluski, P. Coric, V. Thery, W. Gonzalez, H. Meudal, S. Turcaud, J.-B. Michel, B.P. Roques, J. Med. Chem. 39 (1996) 2594–2608.
- [15] R. Bohacek, S. De Lombaert, C. McMartin, J. Priestle, M. Grütter, J. Am. Chem. Soc. 118 (1996) 8231–8249.
- [16] J. Bralet, J.-C. Schwartz, Trends Pharmacol. Sci. 22 (2001) 106–109.
- [17] J.D. Belluzzi, N. Grant, V. Garsky, D. Sarantakis, C.D. Wise, L. Stein, Nature 260 (1976) 625–626.
- [18] B.P. Roques, M.-C. Fournié-Zaluski, E. Soroca, J.M. Lecomte, B. Malfroy, C. Llorens, J.-C. Schwartz, Nature 288 (1980) 286–288.
- [19] C. Oefner, A. D'Arcy, M. Hennig, F.K. Winkler, G.E. Dale, J. Mol. Biol. 296 (2000) 341–349.
- [20] P.R. Gerber, K. Müller, J. Comput.-Aided Mol. Des. 9 (1995) 251–268 (Gerber Molecular Design (<http://www.moloc.ch/>)).
- [21] S.R. Hoertner, T. Ritschel, B. Stengl, C. Kramer, W.B. Schweizer, B. Wagner, M. Kansy, G. Klebe, F. Diederich, Angew. Chem. Int. Ed. 46 (2007) 8266–8269.
- [22] C. Baumgartner, C. Eberle, F. Diederich, S. Lauw, F. Rohdich, W. Eisenreich, A. Bacher, Helv. Chim. Acta 90 (2007) 1043–1068.
- [23] A.K.H. Hirsch, S. Lauw, P. Gersbach, W.B. Schweizer, F. Rohdich, W. Eisenreich, A. Bacher, F. Diederich, ChemMedChem 2 (2007) 806–810.
- [24] R. Siegrist, M. Zürcher, C. Baumgartner, F. Diederich, S. Daum, G. Fischer, C. Klein, M. Dangl, M. Schwaiger, Helv. Chim. Acta 90 (2007) 217–259.
- [25] A. Hoffmann-Röder, E. Schweizer, J. Egger, P. Seiler, U. Obst-Sander, B. Wagner, M. Kansy, D.W. Banner, F. Diederich, ChemMedChem 1 (2006) 1205–1215.
- [26] E. Schweizer, A. Hoffmann-Röder, K. Schärer, J.A. Olsen, C. Fäh, P. Seiler, U. Obst-Sander, B. Wagner, M. Kansy, F. Diederich, ChemMedChem 1 (2006) 611–621.
- [27] S. Sahli, B. Stump, T. Welti, W.B. Schweizer, F. Diederich, D. Blum-Kaelin, J.D. Aebi, H.-J. Böhm, Helv. Chim. Acta 88 (2005) 707–730.
- [28] S. Sahli, B. Stump, T. Welti, D. Blum-Kaelin, J.D. Aebi, C. Oefner, H.-J. Böhm, F. Diederich, ChemBioChem 5 (2004) 996–1000.
- [29] S. Sahli, B. Frank, W.B. Schweizer, F. Diederich, D. Blum-Kaelin, J.D. Aebi, H.-J. Böhm, C. Oefner, G.E. Dale, Helv. Chim. Acta 88 (2005) 731–750.
- [30] K. Müller, C. Faeh, F. Diederich, Science 317 (2007) 1881–1886.
- [31] J.A. Olsen, D.W. Banner, P. Seiler, U. Obst-Sander, A. D'Arcy, M. Stihle, K. Müller, F. Diederich, Angew. Chem. Int. Ed. 42 (2003) 2507–2511.
- [32] J. Olsen, P. Seiler, B. Wagner, H. Fischer, T. Tschopp, U. Obst-Sander, D.W. Banner, M. Kansy, K. Müller, F. Diederich, Org. Biomol. Chem. 2 (2004) 1339–1352.
- [33] C.-Y. Kim, J.S. Chang, J.B. Doyon, T.T. Baird Jr., C.A. Fierke, A. Jain, D.W. Christianson, J. Am. Chem. Soc. 122 (2000) 12125–12134.
- [34] W.R. Dolbier Jr., J. Fluorine Chem. 126 (2005) 157–163.
- [35] D. O'Hagan, H.S. Rzepa, Chem. Commun. (1997) 645–652.
- [36] B.E. Smart, J. Fluorine Chem. 109 (2001) 3–11.
- [37] S. De Lombaert, L.B. Stamford, L. Blanchard, J. Tan, D. Hoyer, C.G. Diefenbacher, D. Wei, E.M. Wallace, M.A. Moskal, P. Savage, A.Y. Jeng, Bioorg. Med. Chem. Lett. 7 (1997) 1059–1064.
- [38] N. Inguimbert, P. Coric, H. Poras, H. Meudal, F. Teffort, M.-C. Fournié-Zaluski, B.P. Roques, J. Med. Chem. 45 (2002) 1477–1486.
- [39] D.A. Evans, D.J. Mathre, W.L. Scott, J. Org. Chem. 50 (1985) 1830–1835.
- [40] K.M. Carvalho, G. Boileau, A.C.M. Camargo, L. Juliano, Anal. Biochem. 237 (1996) 167–173.
- [41] E.A. Meyer, R.K. Castellano, F. Diederich, Angew. Chem. Int. Ed. 42 (2003) 1210–1250.
- [42] C. Allot, H. Adams, P.L. Bernard Jr., C.A. Hunter, C. Rotger, J.A. Thomas, Chem. Commun. (1998) 2449–2450.
- [43] H. Adams, S.L. Cockroft, C. Guardigli, C.A. Hunter, K.R. Lawson, J. Perkins, S.E. Spey, C.J. Urch, R. Ford, ChemBioChem 5 (2004) 657–665.
- [44] H.-J. Böhm, D. Banner, S. Bendels, M. Kansy, B. Kuhn, K. Müller, U. Obst-Sander, M. Stahl, ChemBioChem 5 (2004) 637–643.
- [45] J.S. Lai, E.T. Kool, J. Am. Chem. Soc. 126 (2004) 3040–3041.
- [46] C. Oefner, B.P. Roques, M.C. Fournié-Zaluski, G.E. Dale, Acta Crystallogr. Sect. D: Biol. Crystallogr. 60 (2004) 392–396.
- [47] M. Morgenthaler, E. Schweizer, A. Hoffmann-Röder, F. Benini, R.E. Martin, G. Jaeschke, B. Wagner, H. Fischer, S. Bendels, D. Zimmerli, J. Schneider, F. Diederich, M. Kansy, K. Müller, ChemMedChem 2 (2007) 1100–1115.
- [48] J.D. Dunitz, R. Taylor, Chem. Eur. J. 3 (1997) 89–98.
- [49] M. Morgenthaler, ETH Dissertation No. 17228, Zurich, 2007.
- [50] Molecular graphics images were produced using the UCSF Chimera package from the Resource for Biocomputing, Visualization, and Informatics at the University of California, San Francisco (supported by NIH P41 RR-01081). <http://www.cgl.ucsf.edu/chimera>.